PARTIAL COMPOSITE ACTION OF CONTINUOUS COMPOSITE STEEL GIRDERS STRENGTHENED WITH CFRP

BY

ANAS MOHAMMAD AHMAD DARWISH

A Thesis Presented to the

DEANSHIP OF GRADUATE STUDIES

KING FAHD UNIVERSITY OF PETROLEUM & MINERALS

DHAHRAN, SAUDI ARABIA

In Partial Fulfillment of the

Requirements for the Degree of

MASTER OF SCIENCE

In

CIVIL ENGINEERING

MAY 2015

KING FAHD UNIVERSITY OF PETROLEUM & MINERALS

DHAHRAN- 31261, SAUDI ARABIA

DEANSHIP OF GRADUATE STUDIES

This thesis, written by **ANAS MOHAMMAD DARWISH** under the direction his thesis advisor and approved by his thesis committee, has been presented and accepted by the Dean of Graduate Studies, in partial fulfillment of the requirements for the degree of **MASTER OF SCIENCE IN CIVIL ENGINEERING.**

Prof. AL-Farabi M. Sharif
(Advisor)

Dr. Omar A. Al-Swailem
Department Chairman (A)

Prof. Mohammad H. Baluch
(Member)

Prof. Salam A. Zummo
Dean of Graduate Studies

Prof. Abul K. Azad
(Member)

8/6/15

Date

بسم الله الرحمن الرحيم

(قُلْ إِنَّ صَلاَتِي وَنُسُكِي وَمَحْيَايَ وَمَمَاتِي لِلّهِ رَبِّ الْعَالَمِين)

صدق الله العظيم

Dedicated to

My Beloved Parents

My Brothers

My Sisters

My Friends

My Holy Homeland Palestine

ACKNOWLEDGMENTS

In the name of Allah, the Most Gracious and the Most Merciful Alhamdulillah, all praises to Allah for the strengths and His blessing in completing my MS thesis.

I wish to express my sincere thanks to King Fahd University of Petroleum and Minerals for providing me with all the necessary facilities and support for this research.

I acknowledge, with immense gratitude, for my thesis advisor Prof Al-Farabi M. Sharif for his guidance, attention, and patience. I am deeply appreciation to my committee members, Prof. Mohammed Baluch, Prof. Abul Kalam Azad for their encouragement and insightful comments.

My deepest gratitude goes to my beloved parents for the unceasing encouragement, support and attention. I am also grateful to my sisters and brothers who supported me through this venture.

Sincere thanks to all my friends for their kindness and moral support during my study. Thanks for the friendship and memories. I also place on record, my sense of gratitude to one and all, who directly or indirectly, have lent their hand in this venture.

TABLE OF CONTENTS

LIST OF TABLES

LIST OF FIGURES

ABSTRACT

Full Name : Anas Mohammad Darwish

Thesis Title : Partial Composite Action of Continuous Composite Steel Girders Strengthened with CFRP

Major Field : Civil Engineering

Date of Degree : May 2015

Composite steel-concrete girders are commonly used in bridges and buildings. The composite girder depends mainly on the composite action between steel beam and concrete slab. Composite action forms by providing shear connectors between steel beam and concrete slab. Shear connectors can be contributed to maintain the composite action and prevent the interface slip between steel beam and concrete slab. The composite action level depends on the amount of the transferred tangential shear force. In continuous composite girders, negative moment at interior supports region will generate tensile stress in concrete slab. Composite action between concrete slab and steel beam may lose under the effect of tensile stresses causing cracks of concrete slab. Consequently, CFRP sheets are bonded to the top of concrete slab to maintain the composite action at negative moment region.

This research evaluates experimentally and numerically the performance of continuous composite girders with different shear studs spacing at the negative moment region. The behavior of continuous composite girders is studied with presence of CFRP sheets bonded to the top of concrete slab at negative moment region. The study focused on the interface slip between steel beam and concrete slab, composite girder deflection and stiffness, CFRP stress and girder ultimate load capacity.

ملخص الرسالة

الاسم الكامل: انس محمد دريش

عنوان الرسالة: الكمرات المستمرة المركبة جزئيا والمقوية باستخدام البوليمرالمدعم بألياف الكربون

التخصص: هندسة مدنية (انشاءات)

تاريخ الدرجة العلمية: شعبان 1436هـ

تستخدم الكمرات المركبة من الفولاذ والخرسانة في الجسور والابنية بشكل شائع. حيث تعتمد الكمرات المركبة بشكل أساسي على التأثير المركب ما بين الفولاذ والخرسانة. هذا التأثير يتشكل من خلال وصلات فولاذية ما بين الحديد والخرسانة. يمكن لهذه الوصلات الفولاذية المحافظة على قوة الكمرات المركبة ومنع الإنزلاق ما بين الكمرة الفولاذية والبلاطة الخرسانية، حيث أن فعالية هذه الوصلات تعتمد على مقدار ما تنقله من قوى القص الأفقية. في الكمرات المستمرة المركبة، العزم السالب فوق الدعامات الداخلية يولد قوى شد على البلاطة الخرسانية حيث أن هذه القوى تؤدي إلى فقدان الترابط ما بين الحديد والخرسانة بسبب الشقوق المتشكلة في البلاطة الخرسانية. ونتيجة لذلك، تثبت صفائح من البوليمر المدعم بألياف الكربون على سطح البلاطة الخرسانية للمحافظة على التأثير المركب ما بين الفولاذ والخرسانة في منطقة عزم الدوران السالب.

هذا البحث يهدف الى تقييم أداء الكمرات المستمرة المركبة عمليا ونمذجيا من خلال تركيب وصلات فولاذية على مسافات مختلفة في منطقة العزم السالب، بالإضافة إلى تثبيت صفائح البوليمر المدعم بالكربون على سطح البلاطة الخرسانية في منطقة عزم الدوران السالب. البحث سيركز على دراسة الإنزلاق ما بين الفولاذ والخرسانة، انحراف وصلابة الكمرات المركبة، القوى في صفائح البوليمر المدعم بالكربون وقوة التحمل في الكمرات.

CHAPTER 1

INTRODUCTION

1.1 General

Composite steel-concrete construction has been used since 1930s. The idea was developed by using steel framing system in supporting cast-in-place concrete slabs. It was used by neglecting the bond between concrete slab and steel beam. With the advent of welding, it became practical to use shear studs for connecting steel beam with concrete slab. Composite steel-concrete section was firstly used for designing and constructing bridges. Then, composite construction developed and became economical to be used in building construction in early 1960s.

The usage of composite steel-concrete structures reduces construction cost and efficiently utilizes the materials properties. Considering the high compressive strength of concrete and the high tensile strength of steel, composite steel-concrete girders have some advantages i.e. reducing the weight and depth of the steel section in addition to increasing the floor stiffness which gives an opportunity to increase the span length of the member.

Moreover, fire resistance and construction time can be considered as additional advantages of composite construction.

The composite steel-concrete girder depends mainly on the composite action between the steel beam and concrete slab. Composite action forms by providing shear connectors between steel beam and concrete slab, whereas composite action level depends on the amount of the transferred tangential shear force. The components of steel-concrete girders act independently and interface slip occurs under the load effect if there is no connection between them. As a result, a different strain line is developed for each component with neutral axis which acts at the center of gravity for concrete slab and steel beam as shown in Figure 1.1a. On the contrary, when the two components act compositely (full composite action) and sufficient shear studs are provided for resisting the tangential force, two parts work as a single unit and no relative slip occurs between concrete slab and steel beam. As a result, only single strain line is developed which connects at the top of concrete slab with bottom of steel beam as shown in Figure 1.1c. In partial composite action when there are no sufficient shear studs for transferring tangential force, relative slip decreases with respect to first case (no composite interaction). In addition, the neutral axis for the slab comes closer to the beam and that for the beam comes closer to the slab as shown in Figure 1.1b.

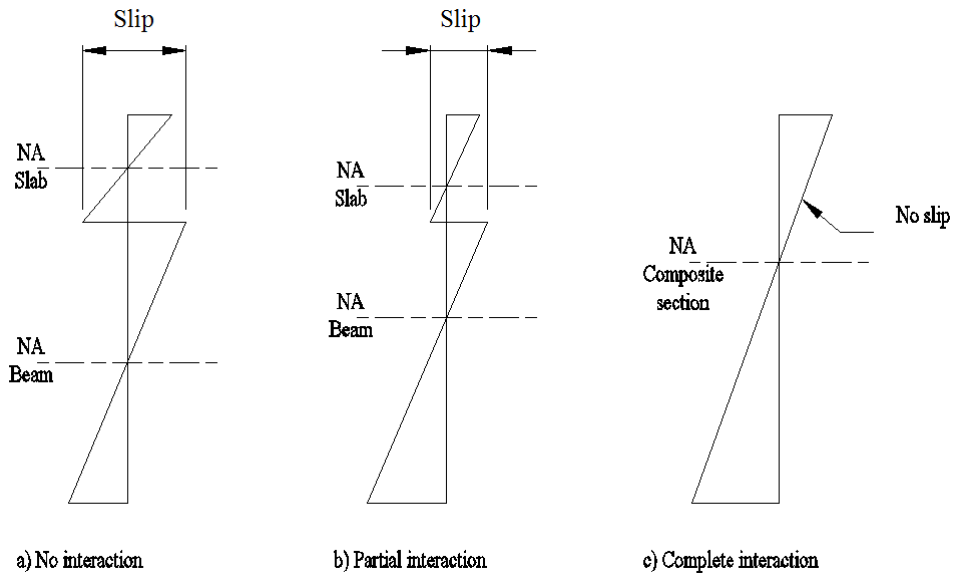

Figure 1.1 Strain variation in composite beam

In continuous composite girders, negative moment at interior support region generates tensile stress in concrete slab. Composite action between concrete slab and steel beam may be lost under the effects of tensile stresses and cracking of the concrete slab, consequently, both strength and stiffness are reduced.

1.2 Shear Connection

As discussed in previous section, the main parameter which affects the composite action between steel beam and concrete slab is the amount of transferred tangential shear force. Depending on that, a full composite or partial composite action is obtained. Mechanical shear connections can be contributed to maintain the composite interaction and

preventing the relative slip and vertical separation between steel beam and concrete slab. AISC (American Institute of Steel Construction) specification provides only two types of shear connection: studs shear connector and channel connectors as shown in Figure 1.2. In recent years, most of the shear connections are headed studs.

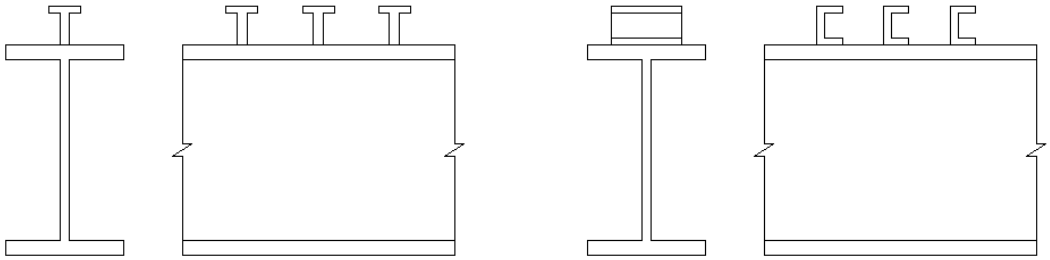

Figure 1.2 Shear connectors types

In full composite action, sufficient shear connection should be provided to produce complete interaction between steel beam and concrete slab. Shear studs should be stiff and rigid enough to prevent any slip at the interface between concrete and steel. In addition, providing enough shear studs enables concrete slab and steel beam to reach their full capacity. In partial composite action, shear capacity for shear studs is insufficient to resist the required interface shear strength. Therefore, the amount of transferred tangential shear force decides the level of composite action. Slip at steel-concrete interface may occur and the shear connections are expected to fail without reaching their full capacity of steel beam and concrete slab.

Transferring of tangential shear force between steel beam and concrete slab can be explained by bearing mechanism. Shear stud deforms and transfers the load to concrete which can cause tensile crack in concrete by ripping, shear, or splitting action as shown in Figure 1.3. Shear stud may also fail before concrete fails. Many researches have showed that the bearing stress is concentrated at the base of shear stud. Also, it has been found that the bearing resistance of concrete on the connector is several times higher than the cylinder strength. This high strength is due to the laterally confinement from steel element, reinforcement and surrounding concrete.

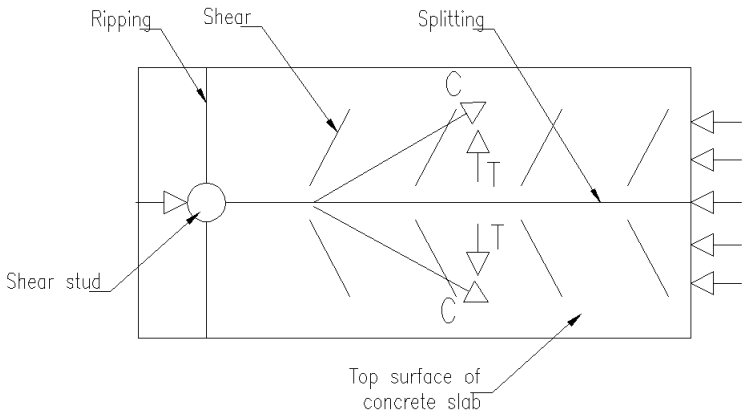

Figure 1.3 Plan view of slab showing crack formation

The required number of shear studs and spacing are varied depending on the value of tangential shear force. This value changes according to loading situation and span length. But the nominal shear transfer strength cannot exceed the maximum force the concrete can develop.

$$C_{max} = 0.85 f_c' b_E t_s \tag{1.1}$$

where b_E is the effective slab width and t_s is the slab thickness. Moreover, when tension force is developed in steel section is less than the compressive force in concrete slab, the maximum shear transfer strength will be

$$T_{max} = A_s F_y \tag{1.2}$$

where A_s is the cross-sectional area of the steel section. Thus, the number of shear studs is equal the compression or tension force divided by the nominal strength of shear connector. It is uniformly distributed between the maximum and zero moment locations.

According to the AISC specifications, shear strength capacity of shear studs mainly depends on the cross-sectional area of shear stud and the properties of concrete. The nominal strength of shear studs Q_n is equal to

$$Q_n = 0.5 A_{sc} \sqrt{f_c' E_c} \tag{1.3}$$

where A_{sc} is the cross-sectional area of shear stud. In addition, shear studs capacity can be determined experimentally using push out test according to Eurocode-4 (2005). More details about this test have been provided in Section 3.3.4.

In continuous composite beam, concrete slab is neglected at negative moment region where concrete is subjected to tensile force. Steel reinforcement can be assumed acting

compositely with steel beam at negative moment region. The maximum tangential shear force that can be transferred by shear studs is

$$T_{max} = A_{S.R}\, F_{y\ S.R} \tag{1.4}$$

where $A_{S.R}$ is the total area of longitudinal reinforcing steel at the interior support, and $F_{y.S.R}$ is the yielding strength of the longitudinal reinforcing steel.

When Carbon Fiber Reinforced Polymer (CFRP) is used for maintaining the composite action at negative moment region, the tensile force developed in CFRP should also be transferred by shear studs. The maximum tangential shear force defined in equation (1.4) becomes

$$T_{max} = A_{S.R}\, F_{y\ S.R} + A_{CFRP}\, \varepsilon_{CFRP}\, E_{CFRP} \tag{1.5}$$

Where A_{CFRP} is the total area of CFRP layers at the interior support, ε_{CFRP} is the strain developed in CFRP, and E_{CFRP} is the elastic modulus of CFRP. The number of shear studs is equal the tension force divided by the nominal strength of shear connector. It is distributed from interior support to each adjacent inflection point.

1.3 Need for the Research

Many researchers have studied the behavior of composite girders using numerical analysis with experimental verification. Composite girders with different levels of shear connections and different arrangements of shear studs were analyzed under negative moment. They studied the action between the shear stud and concrete slab, beam stiffness and deflection, cracks initiating and distribution, and composite girder capacity. In addition, CFRP sheets were used to maintain the composite action at negative moment region for continuous composite girders. Girders with full composite action at negative moment region were bonded with CFRP sheets to the top of concrete slab. They found that the CFRP has the ability to maintain the composite action at negative moment region.

In this study, continuous composite girders with different shear studs spacing at negative moment region were experimentally and numerically investigated. CFRP sheets bonded to the top of concrete slab at the negative moment region. The effectiveness of CFRP was studied with different shear connection levels and proper design method for shear studs spacing at negative moment region was determined.

1.4 Research Objectives

CFRP fabrics are bonded to the top of concrete slab at the negative moment region for continuous composite girders to:

1. Evaluate experimentally the composite action at the negative moment region by varying shear studs spacing.

2. Evaluate numerically the behavior of the continuous composite girders using ABAQUS software.

1.5 Methodology

This study investigates the performance of CFRP with different shear studs spacing. Proper shear studs spacing at negative moment region was determined to make sure that the CFRP maintained the composite action. It is divided into two main parts: experimental work and numerical analysis.

In experimental part, large scale specimens for continuous composite girders were prepared and strengthened with CFRP sheets at negative moment region. After that, the specimens were tested at KFUPM laboratories and the data was recorded and analyzed. In addition, samples for different materials were prepared and tested according to the universal specifications to define its properties.

In numerical analysis part, three-dimensional finite element models were created using ABAQUS software. The models considered the variable shear studs spacing at negative moment region and CFRP sheets bonded to the top of concrete slab at negative moment region. The results of numerical analysis were discussed and verified with experimental results.

1.6 Scope of this Research

The whole content area is divided into two main topics: experimental work and numerical investigation on continuous composite girder with variable shear studs spacing and presence of CFRP at negative moment region. This study is organized into eight chapters. The first Chapter is an introductory part about composite construction, composite action, and shear connection for a better understanding of the background of this study. In the second Chapter, extensive literature review is carried out to identify the need for this research. In Chapter 3, an experimental work on four continuous composite girders and material testing are described. Design of shear studs at positive and negative moment regions are presented in Chapter 4. Chapter 5 presents and discusses the results of the experimental study. In Chapter 6, numerical investigation for continuous composite girders is described. Finite element results are presented and discussed in Chapter 7. Summary and conclusion are provided in Chapter 8.

CHAPTER 2

LITERATURE REVIEW

2.1 Behavior of Partially Composite Beams under Negative Moment

Loh et al. (2004) performed an experimental work on eight composite beams to investigate their behavior under negative moment. Three specimens were tested under static loading and the others were subjected for repeated loading. The three static specimens were designed with different levels of shear connections (83%, 50%, and 33%) but had similar reinforcement ratio. "Each beam was carefully inverted with the concrete slab facing down. The vertical load was applied on the steel flange as a concentrated force at mid-span. Any out-of-plane movement or sideway was prevented by a frame column on one side and significant lateral bracing on the other", Loh et al. (2004). In static tests, it was observed that the beams with shear connection higher than 50% failure by local buckling while beams with less than 50% failure by connector fracture. The beams with higher level of shear connection had a slightly higher moment capacity with reduction of ductility. At later stages of loading, the stiffness of lower shear connection beams decreased due to concrete cracking and concrete-steel slip. Moreover, the shear connectors slip increases with a decrease in the shear connector level.

Fabbrocino & Pecce (2000) carried out tests on simply supported steel-concrete composite beams subjected to negative moment. This study investigated the influence of slab-profile shear connection on the behaviors of the beams. Three inverted composite beams were tested with different arrangements of shear connectors as shown in Figure 2.1. The beams of Types A and B had the same design interaction level with different arrangements while the beams of Type C were designed according to the partial interaction performance. The results showed that the beams of Types A and B failed due to local buckling while Type C beams failed due to headed studs fracture. Depending on the load-deflection curves, three types have agreement in curves up to yielding load and the post-elastic behavior seems to be dependent on the shear connector arrangement. On the other hand, as the deformation increased, the load capacity of the beams decreased. The beam stiffness is influenced by the connection deformability when concrete slab is cracked.

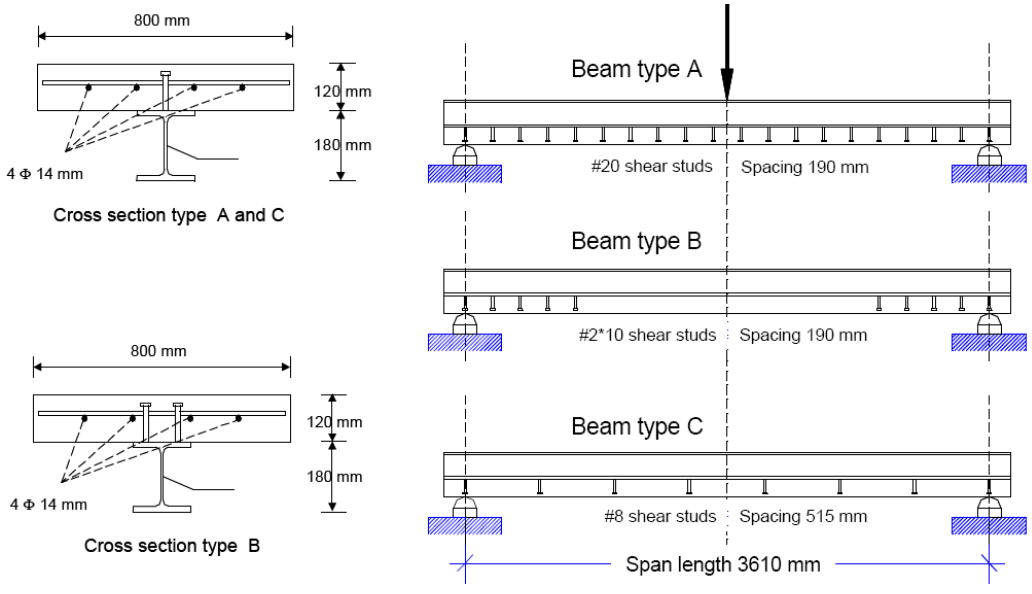

Figure 2.1 Load pattern and the arrangement of connectors, Fabbrocino & Pecce (2000)

Nie et al. (2008) tested 13 steel-concrete composite beams with different levels of shear connections ranged from 25 to 185%. These beams were divided into three different series as shown in Figure 2.2. Series A and B were tested as simply supported beams under positive and negative moments, respectively. Series C was tested as continuous beams with two and three spans. The main parameters considered were the arrangement of shear studs, profiled sheeting, longitudinal reinforcement, and the loading conditions. The tests results for three series are: for Series A, the failure mode depends on the level of shear connection which is governed by studs rupture for specimen with shear connection level less than 50% and by concrete crushing for specimens have more than 50% of shear connections. For Series B, the stiffness of the beams was decreased after the concrete slab cracked. Also, the curvature and deflection increased significantly when the load exceeded 80% of ultimate load. As the shear connection level decreased, the beam capacity and ductility reduced. Cracks developed from the mid-span to the beam end when the load increased. For Series C, the beams behavior was linear up to the first crack developed, after that the length of the cracks increased with increasing load. The cracks reduced the stiffness and capacity of the beam. The specimen's failure was governed by shear studs capacity where all specimens have approximately 50% of shear connection level.

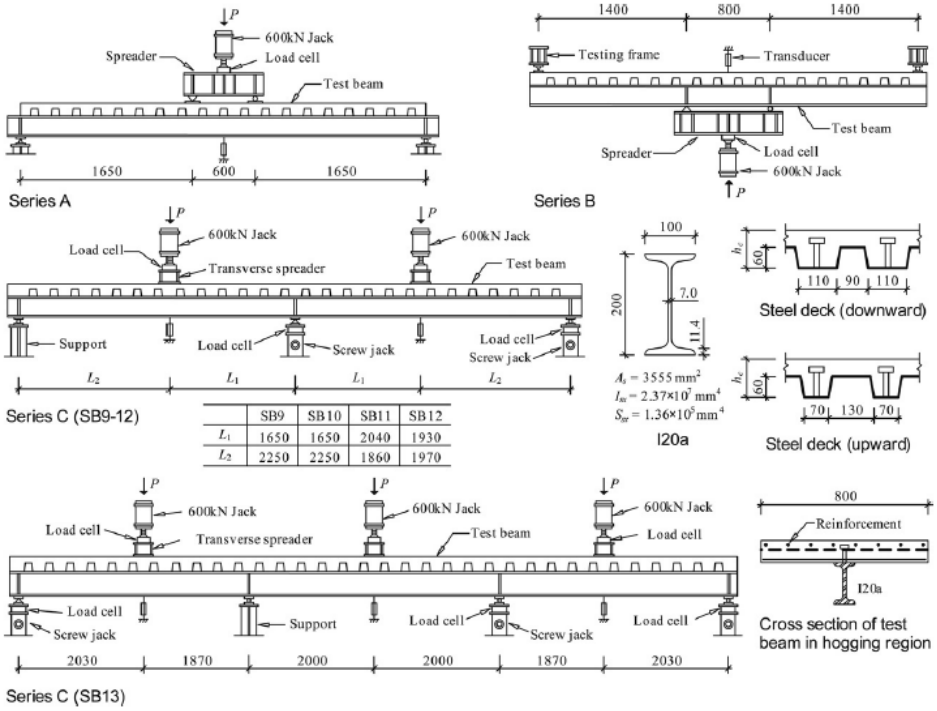

Figure 2.2 Test arrangement, Nie et al. (2008)

2.2 Behavior of Reinforced Concrete Beams with CFRP

Spadea et al. (2001) carried out experimental work on reinforced concrete beams strengthening with CFRP laminates. Eleven plated and unplated beams were divided into three series; these groups have different percentages of longitudinal reinforcement, internal stirrups, and variable location and configuration of external anchorage. The results showed that the load-deflection and moment-curvature response of original beams (without CFRP) were affected by bonding of the CFRP laminates without any external anchorages. The beams with end anchorages produced more ductile failures and carried higher failure load with respect to beams without external anchorage. The bonded CFRP plates increase the beams load capacity and strength, and decrease the deflection and energy absorption.

Nguyen et al. (2001) performed experimental work on ten reinforcement concrete beams, studied their performances with bonded CFRP plates. The plate length, steel ratio, and concrete cover thickness varied their effects on the failure mode and ultimate strength capacity. The beams were tested under four points bending. Four failure modes were observed from the results: flexure failure, shear failure, ripping of concrete and combination between shear and ripping. CFRP-strengthened beams showed considerable increase in strength. The higher increase was found on beams failed in flexural mode while there was smaller increase in beams failed in brittle ripping or combination modes. The bond development length was found to be nearly constant although the beams were reinforced with different lengths of CFRP plates. Concrete ripping could be prevented by limiting the strain at the transition point of the composite of the plate.

Niu & Wu (2006) conducted a finite element model to investigate the effect of interface bond properties on the behavior of reinforced concrete beam strengthened with FRP sheets. A CFRP-strengthened RC beam was analyzed using commercial finite element program DIANA. The performance of RC beams was studied in terms of stiffness, strength, fracture energy, and bond curve shape. It concluded that interfacial stiffness has insignificant effect on the structural stiffness, yield load, and ultimate load capacity. Yield load and ultimate capacity influenced by bond strength where high bond strength increases the effectiveness of FRP strengthen. Interface fracture energy is the main

parameter which affected the yield load, ultimate capacity and ductility. No effect was recorded to local bond shape on the strengthening performance.

2.3 Maintaining Composite Action for Continuous Composite Girders

Basu et al. (1987a) analytically evaluated the behavior of composite steel concrete beams that are pre-stressed at the negative moment region. This study evaluated the effect using pre-stress tendons on concrete cracks at the negative moment region. The results showed that the load carrying capacity increased by 20% and the resultant savings in the size of the beams may offset the extra cost of pre-stressing. The effect of the secondary pre-stressing moment is to reduce the primary pre-stressing moment at the support which became less important with the increase in the number of spans.

Basu et al. (1987b) experimentally studied the behavior of a two-span composite beam consisting of a concrete slab shear connected to a steel beam and pre-stressed near the interior support region. Beam was two spans of 18 ft. and the results were compared with predicted values. According to Basu et al. (1987b), the advantages of partial pre-stressing of composite beams in terms of performance under service loads and economy are further established. The predicted linear and nonlinear response of the two-span partially pre-stressed composite beam up to collapse showed in reasonable agreement with the experimental results, despite the premature local buckling of the bottom flange of the test beam near the interior support. The problem of cracking of the concrete slab and the

resulting partial loss of composite action and stiffness at the negative moment regions of a continuous composite beam can be effectively eliminated by using the proposed partial pre-stressing technique. The test results gave strain values at a section that became nonlinear as the section yielded. The nonlinearity became more pronounced near the central support with the onset of the local buckling phenomenon in the bottom flange.

Chen et al. (2009) carried out an experimental work on continuous composite girders. Four full scale steel-concrete composite girders in two groups with two and three spans were tested. Each group had one non-pre-stressed composite girder and a pre-stressed composite girder with external tendons. The cracking behavior, local buckling and the ultimate strength of the beams were investigated. It was found that the failure was concrete crushing at the positive moment region and web local buckling at the negative moment region. The study showed that a significant increase in the cracking moment resistance was achieved for composite beam pre-stressed with external tendons. The yielding moment at the negative moment region of the beam does not always increase. Lateral, distortional and local buckling occurred in the compression flanges and web of two span composite girders, whether pre-stressed or non-pre-stressed.

Nie et al. (2011) performed a loading capacity analysis for pre-stressed continuous steel-concrete composite girders. Two-span continuous composite girders were analyzed under symmetric concentrated loads to calculate the cracking, yielding, and ultimate capacity of

the girders then extended to general cases. Also, nonlinear finite element model considering the nonlinearity behavior of material and geometry was conducted. The analysis of the model showed the complicity in the behaviors of pre-stressed two-span composite girders during the loading process. Comparisons between experimental and analytical, numerical results showed that the analytical method provided reliable and convenient method for a routine design practice. Finite element model provided excellent numerical simulation for the nonlinear behavior of pre-stressed continuous composite girders.

Sharif & Samaaneh (2014) conducted FE models to investigate the behavior of continuous composite girders under static load and maintaining the fully composite action at negative moment region. Composite girders with CFRP bonded at negative moment region were analyzed. Also, analytical solution using plastic analysis was performed to compare the numerical analysis result. The results showed that the bonded CFRP at negative moment region improved the strength and stiffness of continuous composite girder. Length of CFRP should be extended beyond the inflection points to eliminate premature failure. Plastic analysis conservatively estimated the collapse load.

Sharif & Samaaneh (2015) conducted experimental work on six continuous fully composite girders. The study included the use of CFRP to maintain the composite action at negative moment region. CFRP sheets were bonded to the top of concrete slab at the negative moment region and all girders had full composite action between concrete slab and steel beam. The results showed that the use of CFRP sheets is maintaining the composite action at negative moment region for service load. The bonded CFRP sheets also improved the strength and capacity of the continuous composite girders.

CHAPTER 3

EXPERIMENTAL PROGRAM

3.1 Preparation of Girder

Four continuous steel-concrete composite girders were prepared and tested under one point of loading at the mid of each span. Girders were designed to take into account the capacity of equipment, frames and facilities available in KFUPM labs. The girders were designed also to eliminate local buckling by using proper length/thickness ratio and preventing lateral torsional buckling by using proper cross-section and lateral support at interior support. Shear failure was avoided by using proper web thickness and the flexural failure was required failure at ultimate load.

Preparation of girders took place in three stages. The first stage included manufacturing of steel beam and installation of shear studs. The second stage included casing of concrete slab and the final stage included installation of CFRP sheets at the top of concrete slab. First and second stages were done by contractor outside KFUPM laboratories.

3.1.1 Manufacturing of Steel Beam

In the beginning, steel section parts (web, flanges and stiffeners) were cut from steel sheets with 8mm thickness. These plates were welded together to produce built-up I-section with 5000mm in length and 196mm in depth. In addition, fourteen stiffeners with 180mm in height and 51mm in width were welded at both sides of steel beam, it distributed at the locations of applying the load and the supports. Three steel coupons were also cut from steel sheets for testing and determining the material properties. The dimensions of steel section and longitudinal profile of steel beam are shown in Figure 3.1 and Figure 3.2, respectively. To avoid web local buckling and web crippling, steel plates with 16mm thickness were welded at the bottom flange of supports location.

Afterwards, shear studs with 19mm in diameter and 50mm in length were welded at the top flange. At positive moment region, the four girders had similar shear studs spacing as shown in Figure 3.2. At negative moment region, each girder had different shear studs spacing to produce different levels of composite action. The spacing for shear studs at negative moment region for each girder is summarized in Table 3.1. Figure 3.3 presents the spacing of shear studs at negative moment region during preparation of the girders.

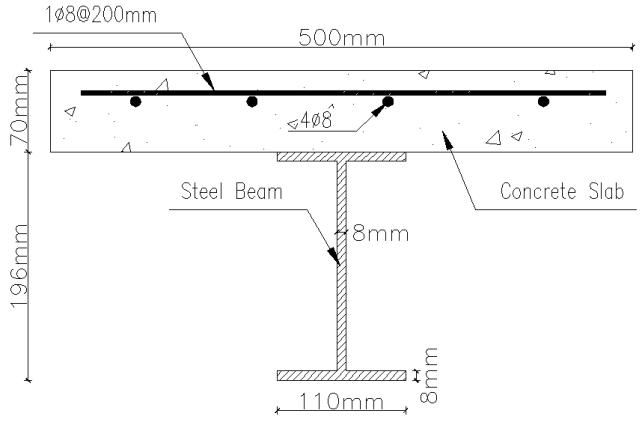

Figure 3.1 Composite girders cross section

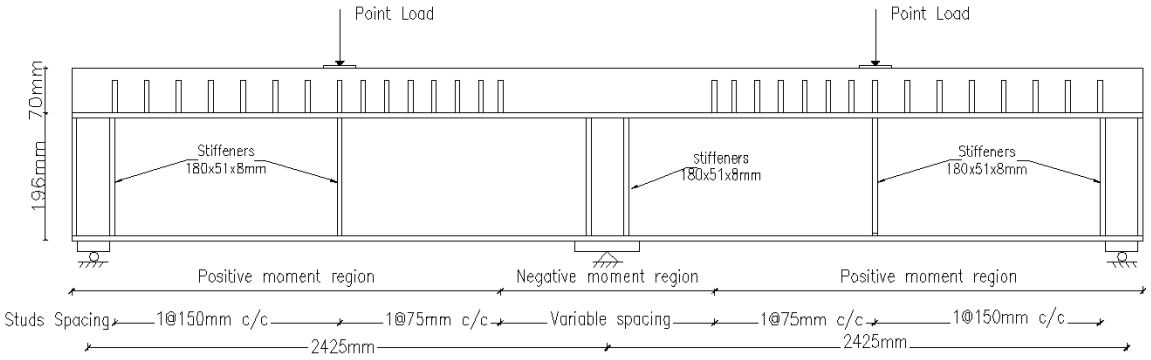

Figure 3.2 Typical specimen dimensions and shear studs spacing

Table 3.1 Shear studs spacing at negative moment region

Specimens	Studs spacing at –ve moment region
G2-16.5R	1@165mm
G2-10R	1@100mm
G2-7.5R	1@75mm
G2-6R	1@60mm

Figure 3.3 Shear studs spacing for each girder at negative moment region

3.1.2 Construction of Concrete Slab

After the finishing of fabrication of steel beam and shear studs, formwork for concrete slab of 500mm in width and 70mm in depth was installed as shown in Figure 3.1. Then, steel reinforcement mesh consisted of four longitudinal bars and a transverse bar was fixed every 200mm inside concrete slab. Steel mesh was installed using plastic spacers to provide suitable concrete cover. Figure 3.4 shows specimen formwork with steel reinforcement. In this stage, four strain gauges were also fixed at upper surface of top flange and on steel reinforcement. It was covered by water proof rubber before casting of concrete slab. Eventually, concrete slab was casted and finishing for slab surface was

completed. Concrete samples of material testing were also taken. Figure 3.5 shows casting process for the specimens.

Figure 3.4 Formwork and steel reinforcement for one of the specimens

Figure 3.5 Casting of specimens

3.1.3 Installation of CFRP Sheets

After the completion of manufacturing process, specimens were delivered to KFUPM labs and specimen's preparation was started for testing. Two layers of Carbon Fiber Reinforced Polymer (CFRP) were bonded at the top surface of concrete slab at negative moment region. Required development length between layers was provided according to ACI-Commetti-440 (2008). Prior the installation of CFRP, concrete surface was treated by sand papers to remove the external loose concrete. In addition, concrete slab under the load at positive moment region was wrapped by one layer of CFRP. The location of CFRP at both negative and moment regions is shown in Figure 3.6.

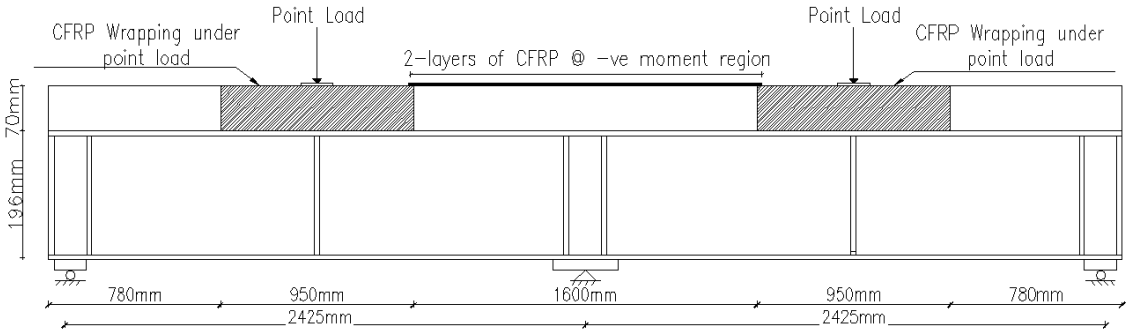

Figure 3.6 CFRP sheets locations

3.2 Testing of Girders

3.2.1 Test Set-up

The experiment was carried out in Heavy Structures Testing Laboratory of King Fahd University of Petroleum and Minerals. Composite girders were tested as two-span continuous beams with 2425mm between supports for each span and five points loading configuration. Load was applied using hydraulic jack and 2000KN load cell at the middle of stiff steel beam HEB450. Load was distributed through the spreader beam into two points at the middle of each span. Each loading point covered the entire slab width and rubber tape was used under the line loads to eliminate any irregularity in the surface. The test set-up schematic is shown in Figure 3.7 while Figure 3.8 shows the test set-up in laboratory.

The specimens were supported by a roller system at the two ends and pin system with lateral supports at the mid of specimen as shown in Figure 3.9 and Figure 3.10, respectively.

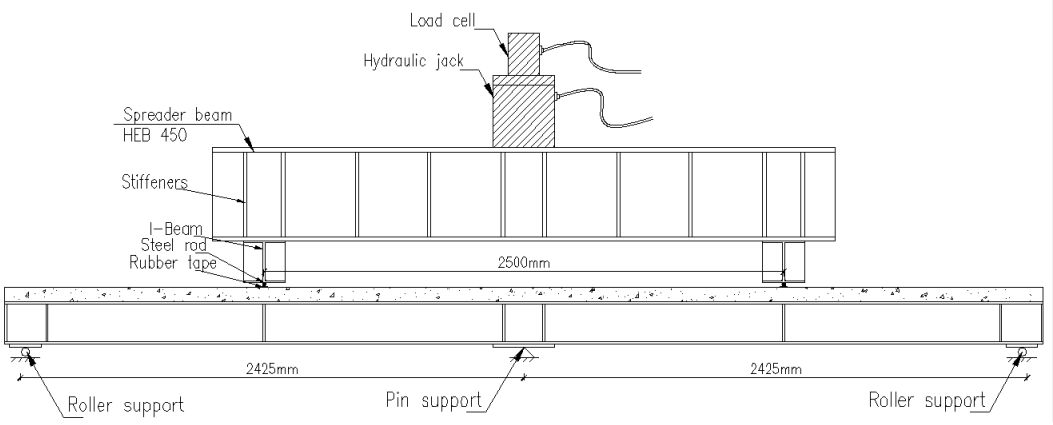

Figure 3.7 Test setup schematic

Figure 3.8 Test set-up in the laboratory

Figure 3.9 Pin and lateral supports system at mid of specimen

Figure 3.10 Roller support system at specimen ends

3.2.2 Instrumentation and Testing

For the purpose of determining strain development through the cross section of specimen, strain gauges were installed at two locations; one at the interior support and the other at mid-span. At each location, thirteen strain gauges were distributed; two strain gauges were fixed at the bottom flange, three strain gauges at the web, two strain gauges at the bottom of concrete slab, and another two at the top of concrete slab. In addition, four strain gauges were installed inside the concrete slab before casting; two strain gauges at the top flange and two at the longitudinal steel reinforcement. The distribution of strain gauges through specimen cross section is shown in Figure 3.11 to Figure 3.13. Moreover, eight strain gauges were fixed along the CFRP sheets, two strain gauges were installed over interior support and two at 250mm, 500mm away from the interior support at both sides.

Two Linear Variable Differential Transducers (LVDTs) were installed at the mid of the two spans to measure vertical deformation; one of these instruments shown in Figure 3.14 while the other was fixed at the top of concrete slab over the interior support to measure crack width. Three LVDTs were fixed in the longitudinal direction between concrete slab and steel beam to measure interface slip as shown in Figure 3.15.

Strain gauges, LVDTs, and load cell were connected to Data Logger for recording data during loading process. Girders were loaded at rate of 30-35KN/min up to failure. Each specimen test was monitored by marking cracks, taking photos, and recording videos. Hence, the data was collected from Data Logger and analyzed.

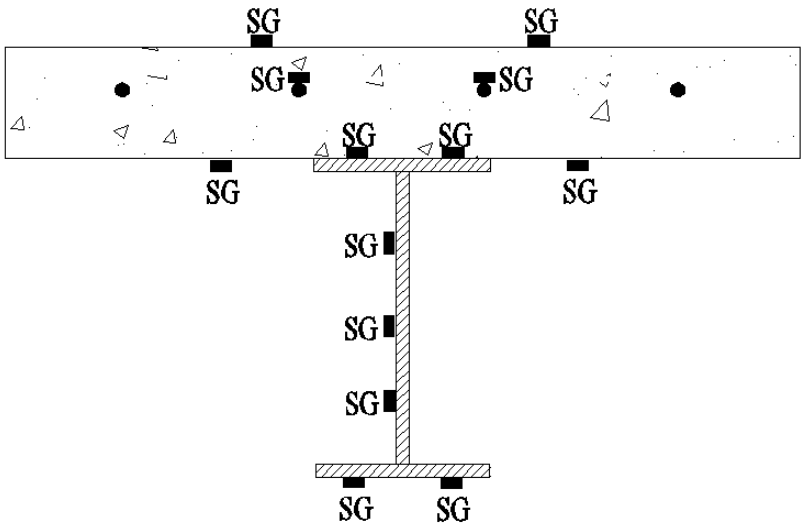

Figure 3.11 Strain gauges distribution at negative and positive moment region

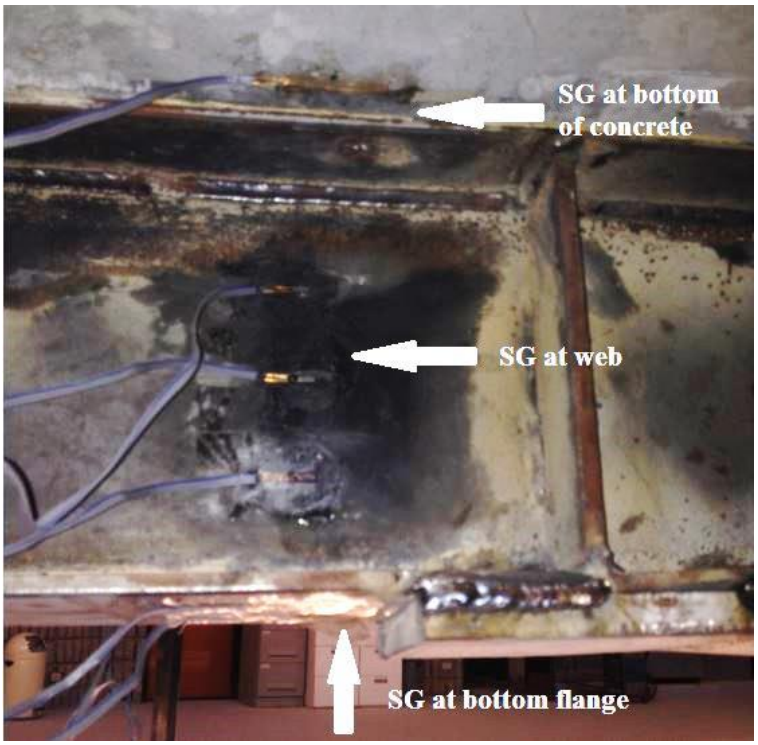

Figure 3.12 Strain gauges distribution through steel section

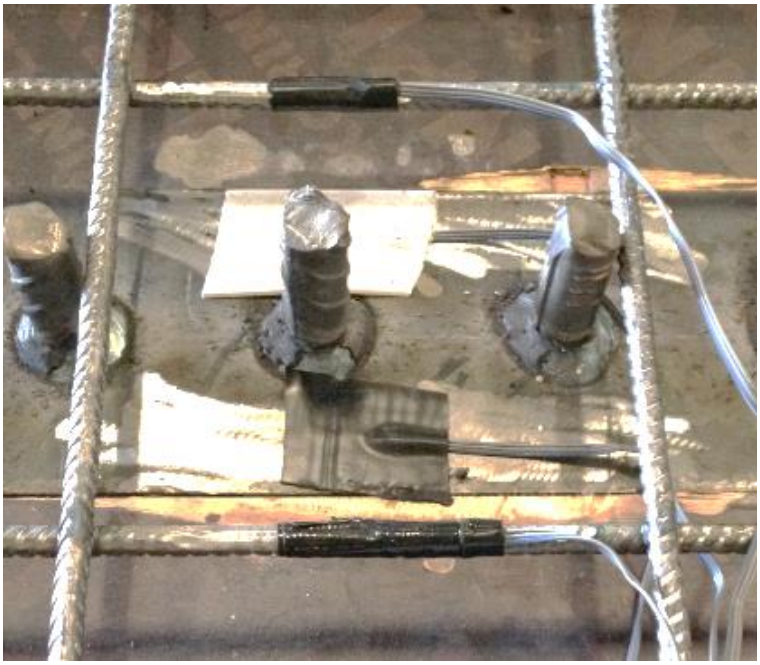

Figure 3.13 Strain gauges with water proof rubber before casting

Figure 3.14 LVDT at mid-span

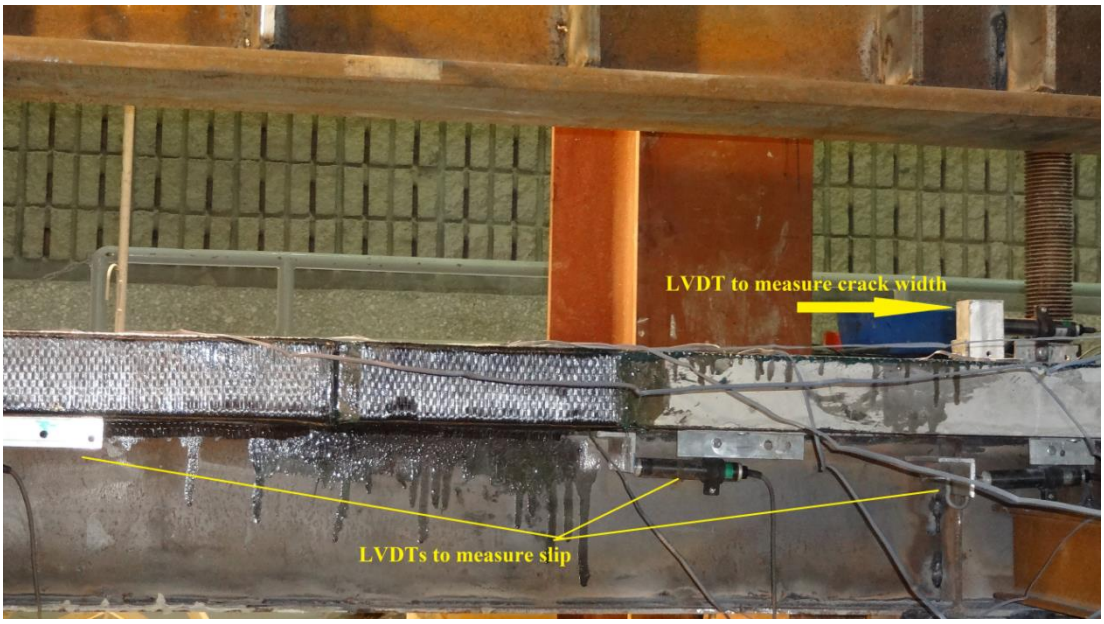

Figure 3.15 LVDTs for measuring slip and crack width

3.3 Material Properties

This section presents the properties of materials used in experimental work, including steel plates, steel reinforcement, concrete, shear studs, and CFRP epoxy.

3.3.1 Steel Plates

For the preparation of steel girders from the steel sheets, three steel coupons were cut and tested according to ASTM E8. Tensile tests were carried out using universal testing machine as shown in Figure 3.16. Two strain gauges were fixed in opposite direction at the center of each plate. Testing machine and strain gauges were connected to Data Logger to record the data. The results of yielding strength, tensile strength and Young's modulus are illustrated in Table 3.1. Also, the stress strain diagram for plates is shown in Figure 3.17.

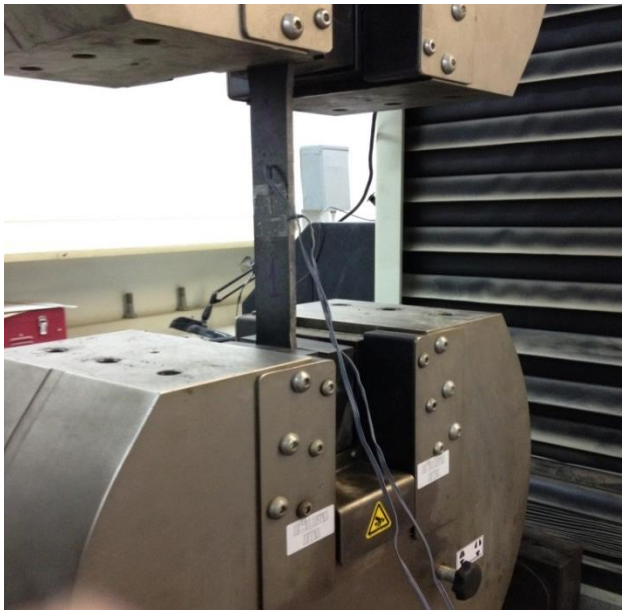

Figure 3.16 Tensile test for steel plate

Table 3.2 Material properties of steel plates

	Yielding Strength (MPa)	Tensile Strength (MPa)	Young's Modulus (GPa)	Poisson's Ratio
Plate-1	284.4	435.9	201.7	0.298
Plate-2	275.0	434.4	203.6	0.299
Plate-3	268.7	430.6	200.6	0.295
Average	**276**	**433.6**	**202**	**0.297**

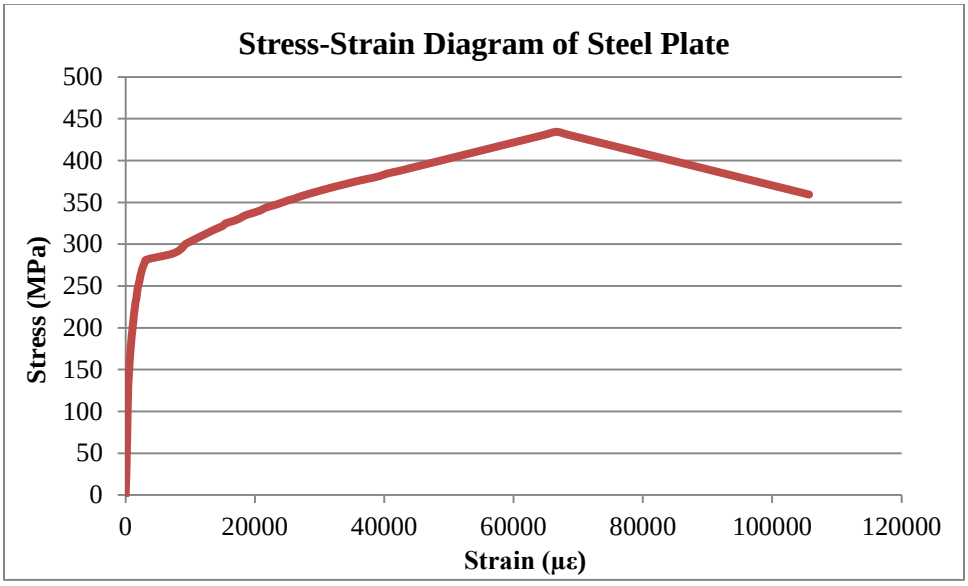

Figure 3.17 Stress-Strain diagrams for steel plates

3.3.2 Reinforcing Bars

Tensile test for reinforcing bars was conducted according to ASTM E8-09. Three samples with 8mm in diameter were tested to determine the property of reinforcing bars as shown in Figure 3.19. The results of yielding strength, tensile strength and Young's modulus are presented in Table 3.3. Also, the stress strain diagram for three samples is presented in Figure 3.18.

Table 3.3 Material property of reinforcing bars

	Yielding Strength (MPa)	Tensile Strength (MPa)	Young's Modulus (GPa)	Poisson's Ratio
Sample-1	417	601	205	0.290
Sample-2	437	585	202	0.293
Sample-3	396	618	209	0.289
Average	**417**	**601**	**205**	**0.291**

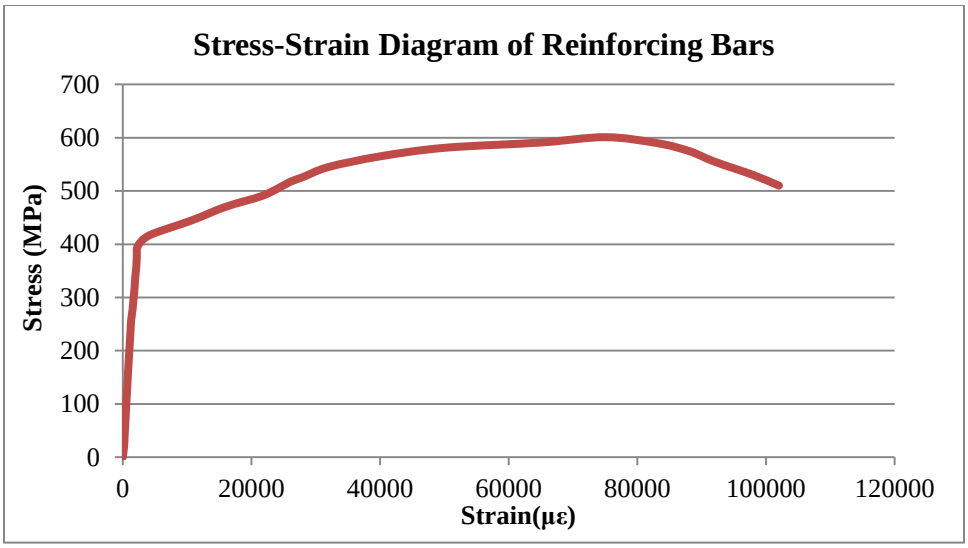

Figure 3.18 Stress-Strain diagram of steel reinforcement

Figure 3.19 Reinforcing bars samples before and after testing

3.3.3 Concrete

3.3.3.1 Compressive Strength and Splitting Tests

Concrete cylinders of 75mm (3 in.) in diameter and 150mm (6 in.) in height were prepared during casting of concrete slab. Compressive strength test was carried out according to ASTM C39-08. Four strain gauges were fixed on each sample of compressive test as shown in Figure 3.20. Measurements of strain gauges were used to draw the relationship between stress and strain during the test as presented in Figure 3.21 and recordings used to calculate the Poisson's ratio for each sample. Splitting test was carried out according to ASTM C496 as shown in Figure 3.22. The splitting tensile strength was calculated as follows:

$$T = 2P/\pi\, l\, d \tag{3.1}$$

where T is the tensile splitting strength, P is the maximum applied load, l is the length of the sample, and d is the diameter of cylinder. The results of compressive and splitting tests' samples are listed in Table 3.4.

Figure 3.20 Set-up of Compressive strength test

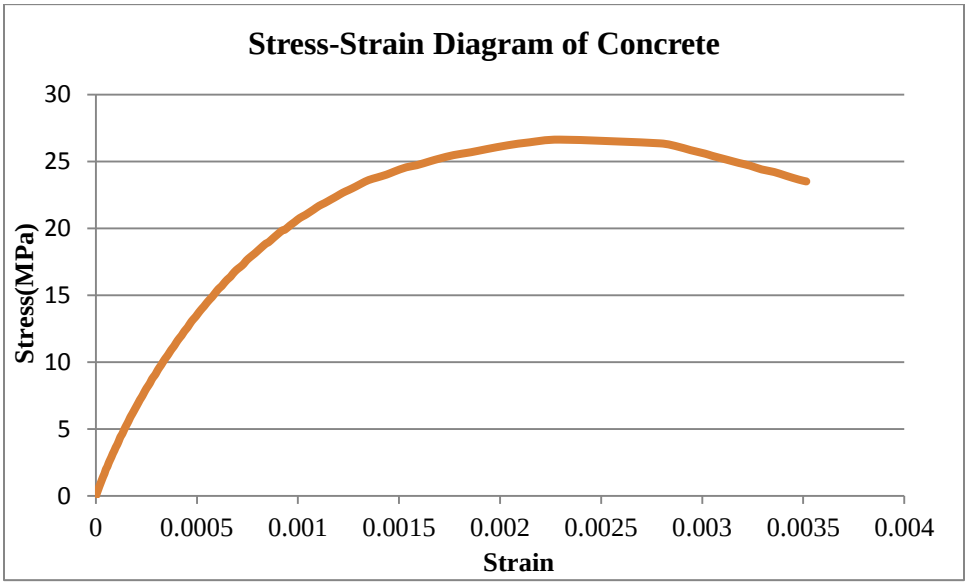

Figure 3.21 Stress-Strain diagram of concrete (Compressive strength test)

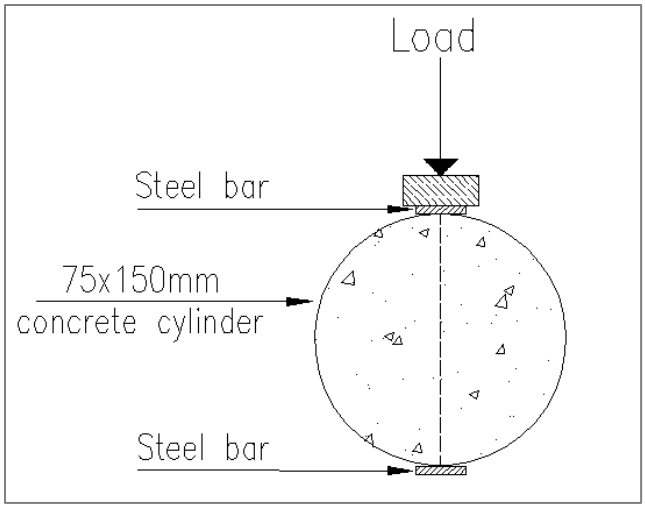

Figure 3.22 Set-up of splitting test

Table 3.4 Results of concrete tests

Compressive Strength Test			Splitting Test	
Sample No.	Compressive Strength (MPa)	Poisson's Ratio	Sample No.	Splitting Tensile Strength (MPa)
CSC-1	27.2	0.191	CSS-1	3.11
CSC-2	26.8	0.190	CSS-2	2.95
CSC-3	26.3	0.217	CSS-3	3.73
Average	**26.8**	**0.199**	**Average**	**3.26**

3.2.3.2 Flexural Test

Six prisms of concrete with dimensions (160x40x40mm) were tested according to ASTM C-293 standards. The test was carried out in three points of loading as shown in Figure 3.23. This test was used to calculate the modulus of rupture as follows:

$$R = 3PL/2bd^2 \tag{3.2}$$

where R is the modulus of rupture, P is the maximum applied load, L is the span length, b is the average width of specimen, and d is the average depth of specimen, at the fracture. The modulus of rupture for the samples was 4.83, 4.25, 4.72, 6.43, 5.45, and 5.90MPa with an average of 5.27MPa.

Figure 3.23 Concrete prism under three points of loading (Flexural test)

3.2.3.3 Cyclic Test

In cyclic test, concrete cylinders were subjected to multiple cycles of loading and unloading. Four strain gauges were fixed at both sides of cylinder as used in compression strength test. Testing machine and strain gauges were connected to Data Logger for monitoring and recording the load and strain data. The results of this test were used for numerical analysis purposes; it was used for damage model parameters in ABAQUS software. Figure 3.24 shows the stress-strain relationship during the test. Also, Figure 3.25 presents the final condition of a sample after the failure.

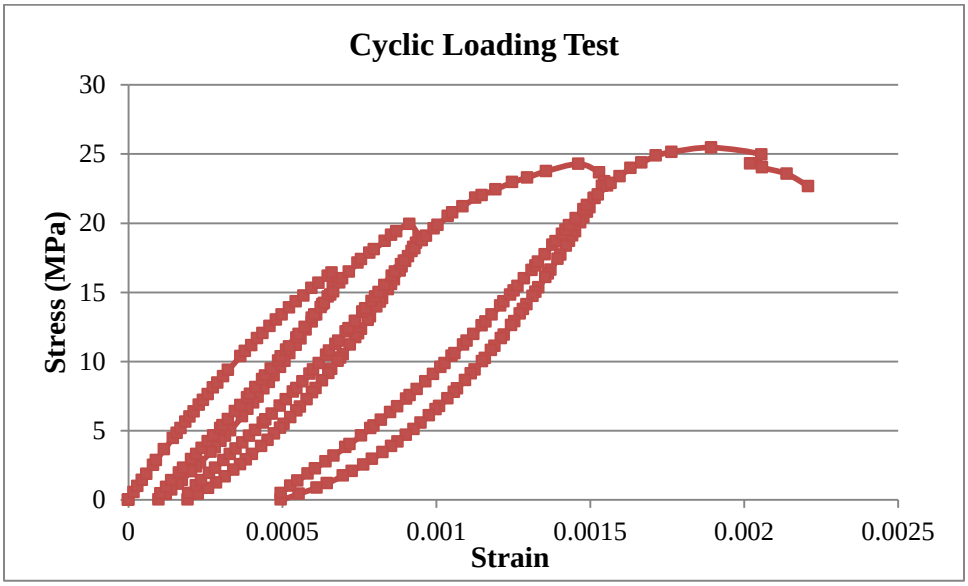

Figure 3.24 Stress-Strain diagram for concrete sample (Cyclic loading test)

Figure 3.25 Concrete cylinder failure after cyclic loading test

3.3.4 Shear Studs

Shear connection between concrete slab and steel beam is the most important factor affecting the composite action. Therefore, determination of shear studs properties is highly significant. Push out test is one of the major tests performed for determining the shear strength capacity and the load-slip characteristics of the shear studs according to Eurocode-4 (2005). There are variables affecting the load-slip relationship, including: number of shear studs in test specimen, mean stress in concrete surrounding the studs, thickness of concrete surrounding the studs, strength of concrete, degree of compaction of

concrete, steel reinforcement arrangement and size, concrete slab support, and bond at the interface between steel beam flanges and concrete slab. On the other hand, the failure mode could by controlled by steel failure (stud yields and fails), concrete failure, and mixed failure between concrete and steel.

As discussed earlier, load-slip curve is one of the main outputs of push out test. It shows the relationship between shear strength capacity of shear stud and average slip. Figure 3.26 shows load-slip relationship for different shear studs; the brittle studs resistance reaches its peak value with relatively small slip then fails suddenly while the ductile studs maintain their shear capacity over large displacement. Connector stiffness k is one of the main parameters that can be obtained from load-slip curve. Figure 3.27 shows an idealized load-slip characteristic based on different types of interaction that can be developed depending on the type of shear connector. It is noted that full interaction occurs when very stiff connectors are used and $k=\infty$. When there is a partial interaction, load slip relationship is assumed to be bilinear and the ultimate capacity is P_{max}. In addition, the stiffness k is assumed to be constant from zero shear loads up to P_{max}.

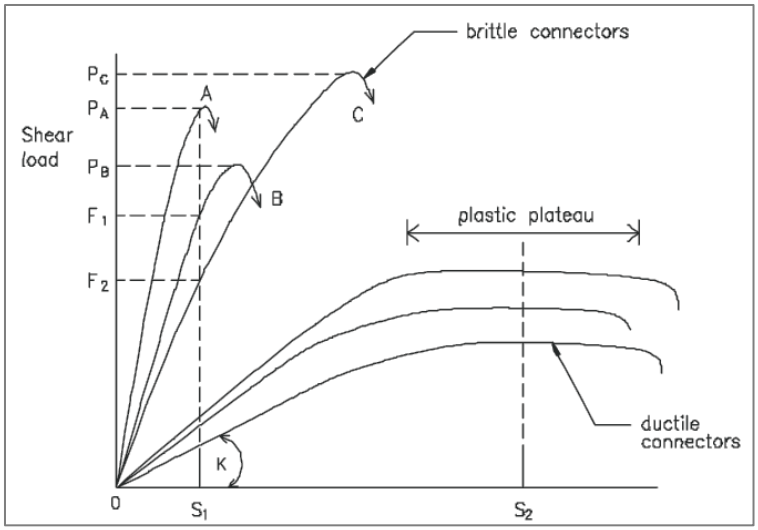

Figure 3.26 Load-slip characteristics

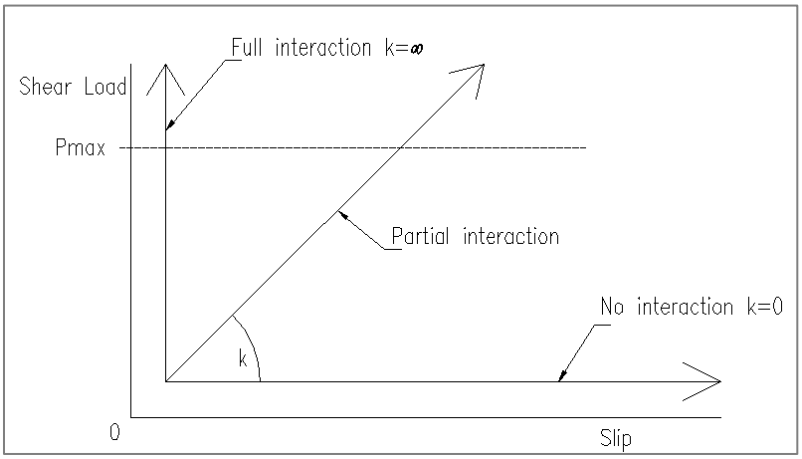

Figure 3.27 Idealized load-slip characteristics

In push out test, shear studs were welded to the flanges of steel beam, steel reinforcement was fixed inside slab formwork, and concrete slabs were horizontally casted. A typical specimen for push out test is shown in Figure 3.28. Concrete slabs were bedded onto the lower platen of testing machine and load was vertically applied at the upper end of steel

section. Further, LVDT was vertically fixed under steel beam to measure vertical displacement during loading process. Test set-up in laboratory shown in Figure 3.29 while Figure 3.30 presents the average load-slip relationship for the tested shear studs. The shear strength capacity and slip capacity of shear studs were calculated according to Eurocode-4 procedure. The shear strength capacity of shear studs is equal to 90% of ultimate load as shown in Figure 3.30 and this value equals 64KN. The slip capacity should be taken as the maximum slip measured at the shear strength capacity as shown in Figure 3.30 and this value equals 1.30mm. The stud stiffness *k* equals 92KN/mm which is calculated as the slope of linear part of the load-slip curve. The failure mode was shear failure for concrete block as shown in Figure 3.31.

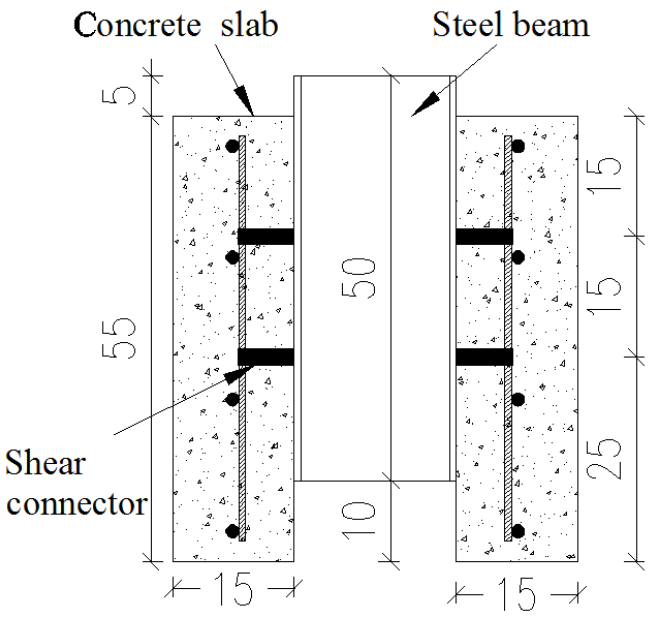

Figure 3.28 Typical push-out test specimen

Figure 3.29 Push-out test set-up in the laboratory

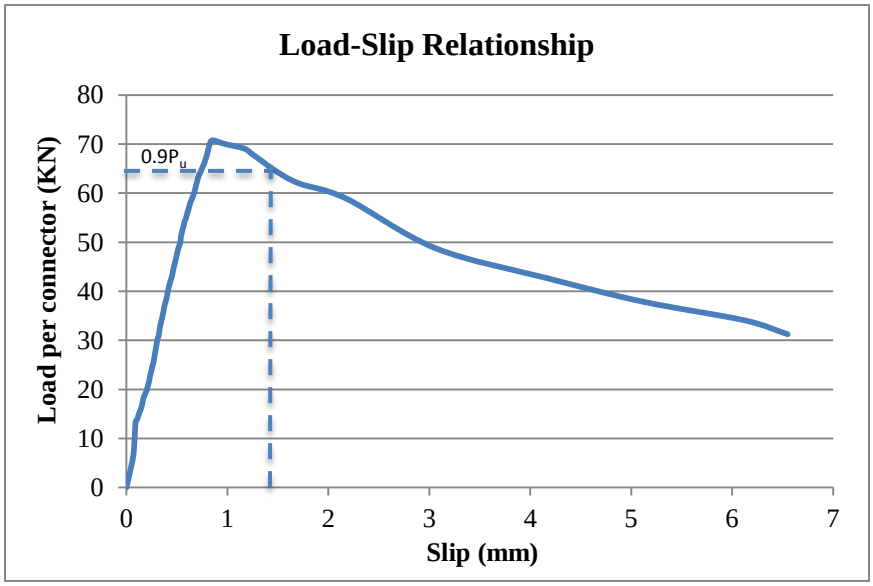

Figure 3.30 Load-slip relationship for shear studs

Figure 3.31 Failure mode of push-out test specimen

3.3.5 Carbon Fiber Reinforced Polymer (CFRP)

CFRP is a high strength and light weight material which is used for strengthening of structures. There are different types of CFRP depending on the matrix composition. In this study, Unidirectional CFRP was used for strengthening the specimens. The properties of CFRP according to Manufacturer are: the fiber density is 1.8g/cm^3, thickness is 0.131mm, ultimate elongation is 1.5%, tensile strength is about 3500MPa, and the elastic modulus is 230GPa.

Adhesive material (Primer) was used for bonding CFRP with concrete and Encapsulation Resin was used for connecting CFRP layers. Each type of epoxy consists of two main parts: base and hardener. The bond between CFRP and concrete was tested. The

experiment specimens were prepared as set-up shown in Figure 3.32. Five strain gauges were fixed along CFRP sheet and bonded area. Two strain gauges were fixed at bonded area to measure slip between the two materials while the other three measured strain in CFRP. This test provided the maximum stress in CFRP up to failure, rupture failure of CFRP or de-bonding. The results were used to plot shear stress vs. slip for epoxy adhesive (Figure 3.33) and stress-strain relationship for CFRP up to de-bonding (Figure 3.34). The epoxy adhesive strength was 2MPa and the failure was de-bonding between concrete and epoxy as shown in Figure 3.35.

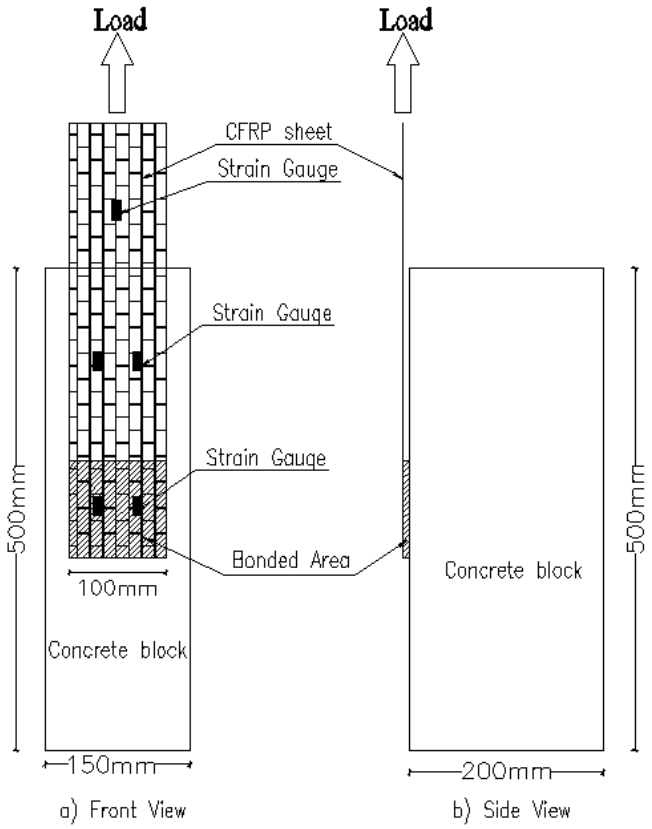

Figure 3.32 Bond test set-up

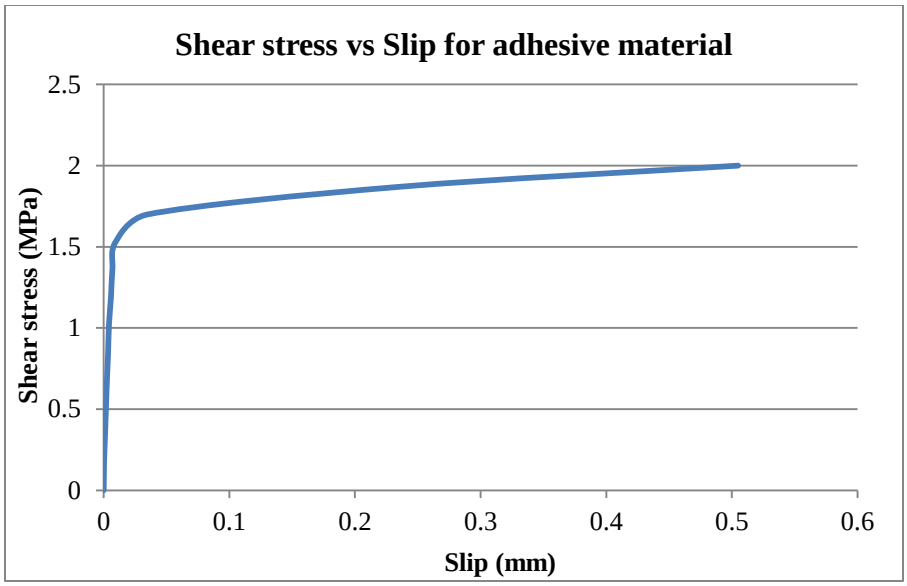

Figure 3.33 Shear stress with slip relationship for adhesive material

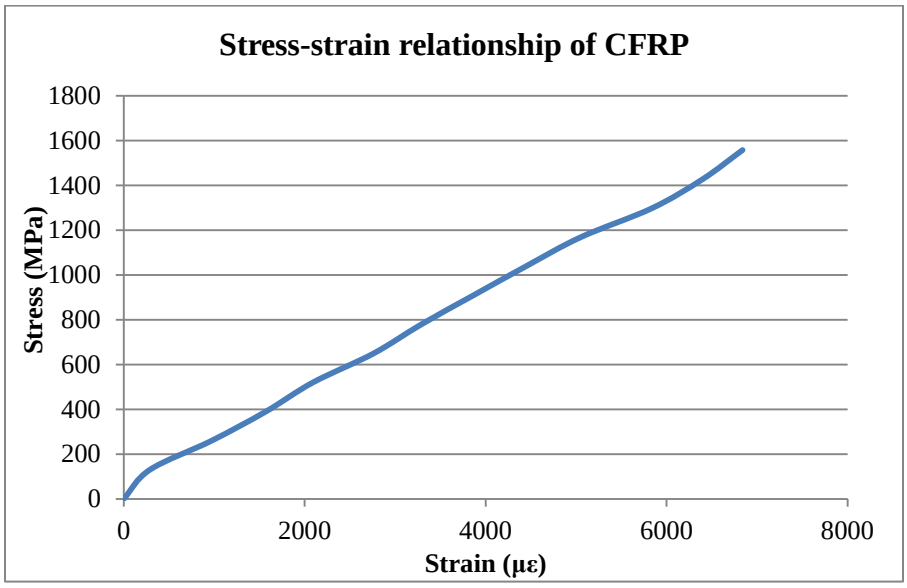

Figure 3.34 Stress-strain relationship of CFRP

Figure 3.35 De-bonding failure in epoxy test

CHAPTER 4

SHEAR STUDS DESIGN

At girders preparation stage, all girders were designed to have full composite action at positive moment region based on assumed material properties. Also, G2-7.5R was designed for full composite action at negative moment region. When actual material properties were determined, shear studs design was revised. The results showed that the girders had partial composite action at positive moment region while G2-7.5R had shear connection level equal to 146% of full composite action at negative moment region. Therefore, G2-10R shifted to represent the full composite girder at negative moment region. Shear studs design for these situations have been discussed in this chapter. Assumed and actual material properties are listed in Table 4.1.

Table 4.1 Material properties

Material / Property	Assumed Material	Actual Material
Concrete compressive strength Fc' (MPa)	28	26.8
Yielding strength of steel plate fy (MPa)	248	276
Yielding strength of steel reinforcement $f_{y\ S.R}$(MPa)	420	417
Shear strength capacity of shear stud (KN)	118	64
Tensile strength of CFRP (MPa)	3500	3500

4.1 Positive Moment Region

4.1.1 Assumed Shear Studs Design

In this section, the design calculations depend on assumed material properties.

Assume the neutral axis N.A in the concrete slab, a < t_s as shown in Figure 4.1.

$C = 0.85\, f_c' b_E\, a \;+\; A_{SR} f_{y\,SR}$

$= 0.85x28x500x(a) + 201x420$

$= 11900a + 84420\ N$

$T = f_y(2b_f t_f + b_w t_w)$

$= 248(2x110x8 + 8x180)$

$= 793600N$

$C = T$

$a = 59.6mm < 70mm \quad OK$

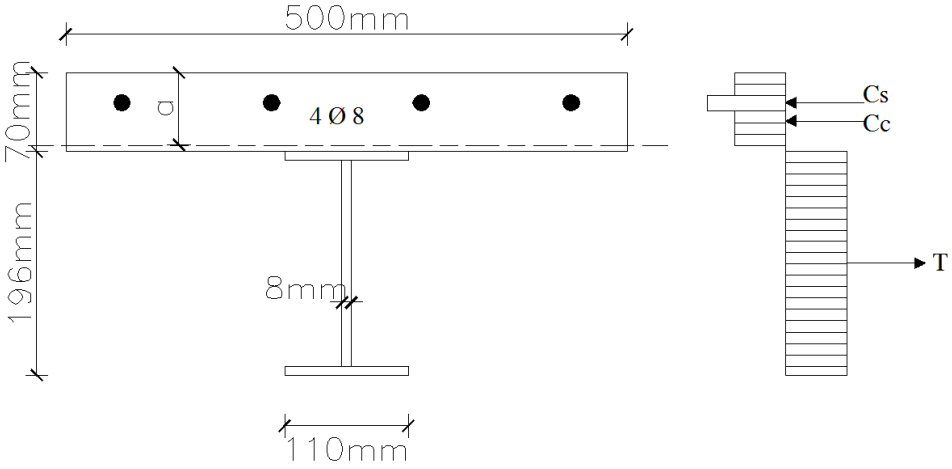

Figure 4.1 Beam cross section at positive moment region

The tangential shear force should be transferred by shear studs is equal to 793.6KN.

According to AISC specifications, shear strength capacity of shear stud is,

$$Q_n = 0.5\, A_{sc} \sqrt{f_c' E_c}$$

$$= 0.5x283.4\sqrt{28x24870}$$

$$= 118KN$$

Number of shear studs= 793.6/118 =7 studs

To define the positive and negative moment regions, firstly, moment capacity was calculated at mid-span and interior support. The moment distribution is shown in Figure 4.3.

At positive moment region;

$$M_{+ve} = 3200x248\left(\left(\frac{196}{2}\right) + 70 - \left(\frac{59.6}{2}\right)\right)$$

$$= 110KN.m$$

$M_{-ve} = 68KN.m$ Detailed calculation will be presented in section 4.2.1.

Location of inflection point from mid-span

$$= \left(\frac{110}{110+68}\right)x1250 = 750mm$$

Shear studs spacing between mid-span and exterior support = 1250/7 ≈ 175mm, it was considered as 150mm conservatively.

Shear studs spacing between mid-span and inflection point = (750)/7 ≈ 105mm, it was considered as 75mm conservatively.

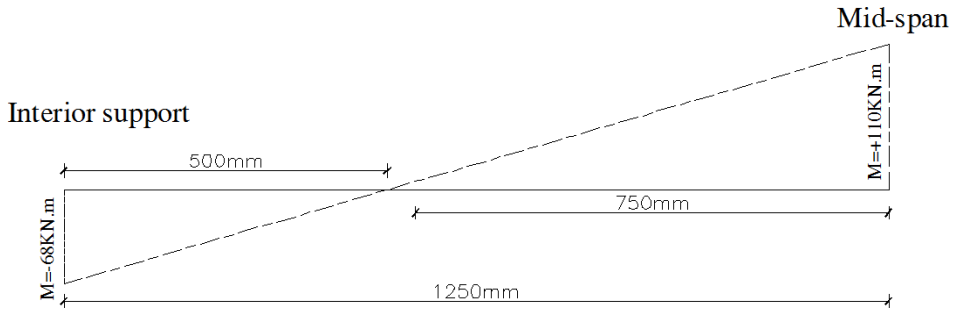

Figure 4.2 Moment distribution between mid-span and interior support

4.1.2 Actual Shear Studs Design

In this section, the design calculations depend on the actual material properties.

Assume the neutral axis N.A in the concrete slab, a < t_s as shown in Figure 4.1

$$C = 0.85\, f_c' b_E\, a + A_{SR} f_{y\,SR}$$

$$= 0.85x26.8x500x(a) + 201x417$$

$$= 11390a + 83817\ N$$

$$T = f_y(2b_f t_f + b_w t_w)$$

$$= 276(2x110x8 + 8x180)$$

$$= 883200N$$

$$C = T$$

$$a \approx 70mm \qquad OK$$

The tangential shear force should be transferred by shear studs is equal to 883KN.

Based on push out test results, the shear strength capacity for shear stud is 64KN.

Number of shear studs= 883/64 =13 studs

To define the positive and negative moment regions, moment capacity was calculated at mid-span and interior support. The moment distribution is shown in Figure 4.3.

At positive moment region;

$$M_{+ve} = 3200x276\left(\left(\frac{196}{2}\right) + 70 - \left(\frac{70}{2}\right)\right)$$

$$= 117KN.m$$

$M_{-ve} = 97KN.m$ Detailed calculation will be presented in section 4.2.2.

Location of inflection point from mid-span

$$= \left(\frac{117}{117+97}\right)x1250 = 700mm$$

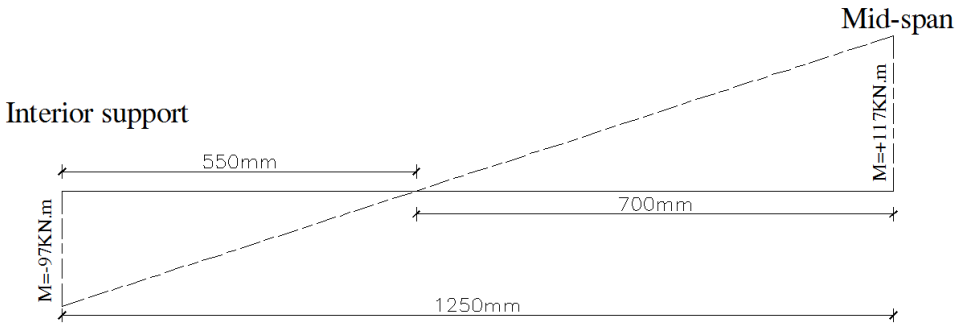

Figure 4.3 Moment distribution between mid-span and interior support

Shear studs spacing between mid-span and exterior support = 1250/13 ≈ 100mm

Shear studs spacing between mid-span and inflection point = (700)/13 ≈ 55mm

Comparison between actual design and available shear studs spacing showed that the shear connection level at positive moment region was partially composite action as

summarized in Table 4.2. Consequently, moment capacity at positive moment region was revised according to the partial composite action design.

Table 4.2 Summary of shear studs design at positive moment region

Region / Item	Mid-span to exterior support	Mid-span to inflection point
Actual shear studs design	1@100mm	1@55mm
Available shear studs	1@150mm	1@75mm
Shear connection level	67%	73%

In partial composite action design, the force in the concrete slab is based on the studs' strength. The average number of shear studs at positive moment regions is nine, ten shear studs between mid-span and exterior support, and eight studs between mid-span and inflection point.

$\Sigma Q_n = 9x64 = 576KN.$

Assume the neutral axis N.A in the top flange as shown in Figure 4.4.

$C = \Sigma Q_n + C_f$

$C = 576000 + 110x(y)x276$

$= 576000 + 30360y$

$T = T_{bf} + T_w + T_{tf}$

$T = (110x8 + 180x8 + 110x(8 - y))x276$

$= 883200 - 30360y$

$C = T$

$y = 5.06mm$ from the top edge of top flange.

Since ΣQ_n representing the shear strength of the shear studs, force ΣQ_n is taken equivalent to C_c+C_{sr}.

$$\Sigma Q_n = 0.85\, f_c' b_E\, a + A_{SR} f_{y\,SR}$$

$$576000 = 0.85x26.8x500x(a) + 201x417$$

$$a = 43.2mm$$

The moment capacity becomes as follow.

First, the centroid of tension region from the bottom of steel section;

$$y_1 = (880x4 + 1440x98 + 323.4x189.47)/2643.4$$

$$= 77.90mm$$

$$M_{+ve} = \Sigma Q_n \left(y + t_s - \frac{a}{2}\right) + C_f \left(\frac{y}{2}\right) + T(d - y - y_1)$$

$$= 576000\left(5.06 + 70 - \left(\frac{43.2}{2}\right)\right) + 153622\left(\frac{5.06}{2}\right) + 729578(196 - 5.06 - 77.9)$$

$$= 113KN.m$$

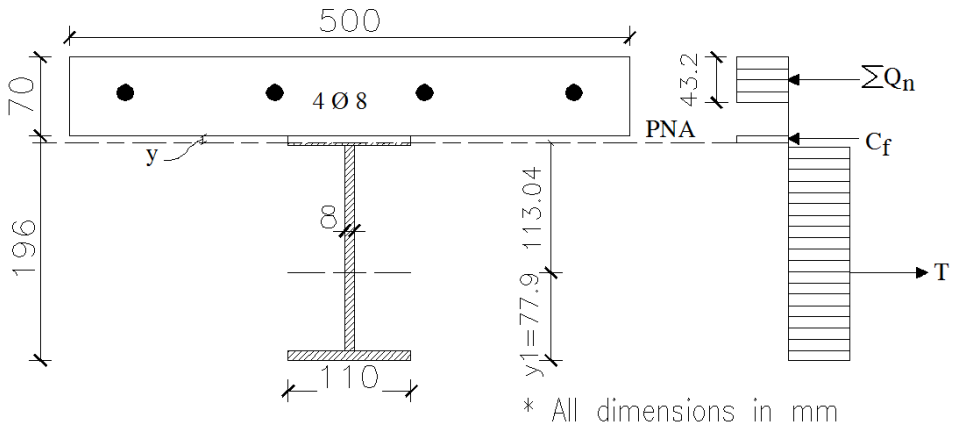

Figure 4.4 Beam cross section at positive moment region (Revised-Partial Case)

4.2 Negative Moment Region

4.2.1 Assumed Shear Studs Design

The tensile strength of concrete was neglected. Shear studs should be transfer tangential force from steel reinforcement and CFRP. It was assumed to use four layers of CFRP with ultimate strain equal to 0.011, thickness of CFRP layer is 0.131mm, and elastic modulus is 230GPa.

$T_{CFRP} = (0.011x230x10^3)x500x4x0.131$

$= 663KN$

$T_{S.R} = 201x420$

$= 84KN$

$Total\ force = T_{CFRP} + T_{S.R}$

$= 747KN$

Number of shear studs= 747/118 =7 studs

To determine negative moment region, moment capacity was calculated depending on the cross section without CFRP as shown in Figure 4.5.

Assume the neutral axis N.A in web,

$C = C_w + C_f$

$C = ((y - 8)x8 + 110x8)x248$

$= 202368 + 1984y$

$T = T_{S.R} + T_w + T_{tf}$

$$T = 201x420 + ((188 - y)8 + 110x8)x248$$

$$= 675652 - 1984y$$

$$C = T$$

$$y = 119.3mm \ \ from\ bottom\ of\ steel\ section$$

$$M_{-ve} = 201x420x111.3 + 248x(110x8x72.7 + 68.7x8x34.4 + 111.3x8x55.7 + 110x8x115.3)$$

$$= 68KN.m$$

Shear studs spacing = (1250-750)/7 =75mm to provide full composite action at negative moment region.

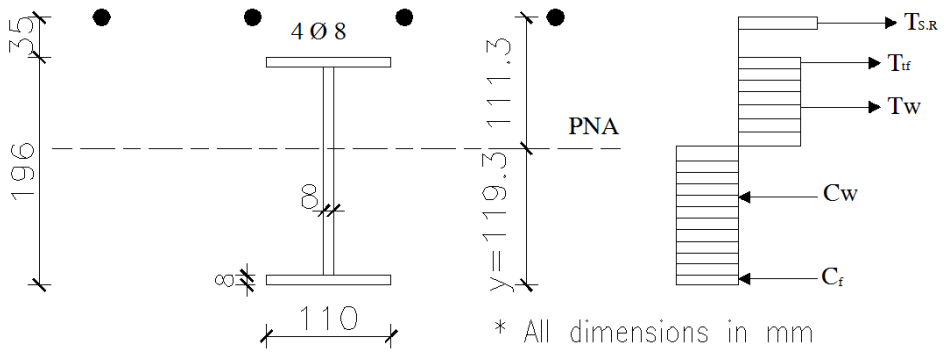

Figure 4.5 Beam cross section at negative moment region (Assumed case)

4.2.2 Actual Shear Studs Design

In this section, the design calculations depend on the actual material properties. The tensile strength of concrete was neglected. Shear studs should be transferred tangential force from steel reinforcement and CFRP where PNA is in steel section as shown in Figure 4.6.

- CFRP strain= 6000με depending on experimental work.

$T_{CFRP} = (0.006x230x10^3)x500x2x0.131$

$= 180KN$

$T_{S.R} = 201x417$

$= 84KN$

$Total\ force = T_{CFRP} + T_{S.R}$

$= 264KN$

Number of shear studs= 264/64 =5 studs

The moment capacity at negative moment region is:

First, assume the neutral axis N.A in the web

$C = C_w + C_f$

$C = \big((y-8)x8 + 110x8\big)x276$

$= 225216 + 2208y$

$T = T_{CFRP} + T_{S.R} + T_w + T_{tf}$

$T = 180000 + 201x420 + ((188-y)8 + 110x8)x276$

$= 922404 - 2208y$

$C = T$

$y = 158mm\ \ from\ bottom\ of\ steel\ section$

$M_{-ve} = 201x417x73 + (110x8 + 150x8)x108.4x275$

$+ (110x8 + 30x8)x29.9x276 + 180000x130$

$= 97\ KN.m$

Shear studs spacing = (1250-700)/5 =110mm.

So, the shear studs spacing required to achieve full composite action at negative moment region is 110mm. Summary of shear studs spacing and composite action level for all girders is presented in Table 4.3.

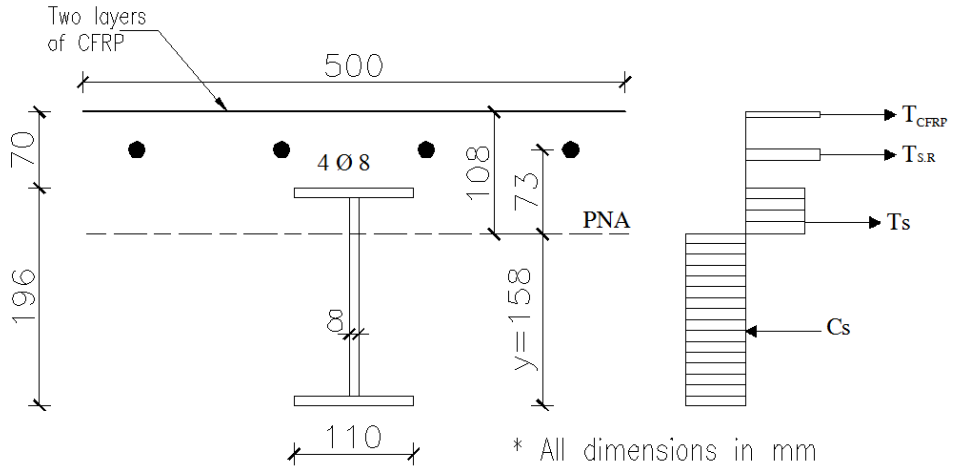

Figure 4.6 Beam cross section at negative moment region

Table 4.3 Summary of shear studs design at negative moment region

Specimens	Studs Spacing at –ve Moment Region	Shear Connection Level
G2-16.5R	1@165mm	66%
G2-10R	1@100mm	110%
G2-7.5R	1@75mm	146%
G2-6R	1@60mm	183%

CHAPTER 5

EXPERIMENTAL RESULTS

This chapter presents the detailed experimental results for four continuous steel-concrete composite girders with variable shear studs spacing at negative moment region and presence of CFRP bonded to the top of concrete slab. The observations and behavior of girders during tests are covered. The effect of shear studs spacing are discussed through load–deflection curve, failure modes, interface slip, and strain distribution. In addition, the performance of CFRP and development of crack width are presented and discussed.

5.1 Load and Deflection Curves

A general look at the relationship between the applied load and deflection at mid-span (Figure 5.1) shows that the girders behave identically with small variation in the stiffness. Girders G2-10R, G2-7.5R, and G2-6R have almost same load-deflection curves while G2-16.5R has slightly less stiffness. Comparison of the cracking load between the girders shows that the cracks appear almost at the same level of loading for all girders. In addition, girders become yielded within short interval of loading (Table 5.1). Also, there is an inconsiderable difference in the ultimate load capacity between different girders. It is concluded from the observations that the shear studs spacing at negative moment region have no clear effect on the loading history of the girders during elastic and plastic stages.

Girders that have full composite action behave less flexible during loading process, but it deflects more at ultimate load compared with partial composite girder. Girders G2-10R, G2-7.5R, and G2-6R have close deflection values at ultimate load. Therefore, the increase of shear connection level more than 100% does not affect the maximum deflection values. Toughness is also calculated to evaluate the effect of shear studs spacing on the performance of the girders. It is equal to the area under load-deflection curve and represents the energy dissipation during loading process. Toughness is increased by reducing shear studs spacing because the girders with lower shear studs spacing reach a bit higher ultimate load and the area under the curve becomes larger. As a conclusion, 100mm shear studs spacing at negative moment region is sufficient to provide acceptable load capacity and deflection. Figure 5.2 shows the deflected shape of specimen G2-10R at ultimate load.

Two failure modes are observed; crushing of concrete slab at mid-span and de-bonding of CFRP at negative moment region (Figure 5.3). The crushing failure mode is due to the concrete strain at mid span reaches its ultimate capacity whereas girders failed by de-bonding of CFRP reach de-bonding strain in CFRP. The interface shear stress between CFRP and concrete is calculated based on analytical model proposed by Rosenboom & Rizkalla (2008). The shear stresses in G2-16.5R, G2-10R, G2-7.5R and G2-6R are equal to 1.90, 1.79, 2.20, and 2.15 N/mm^2, respectively. The detailed calculations of these stresses will be presented in5.4. This means that the shear stress of G2-7.5R and G2-6R exceeds the shear stress capacity of the epoxy according to adhesive material test (2MPa)

as described in Section 3.3.5. Therefore, the de-bonding failure occurred in these two girders.

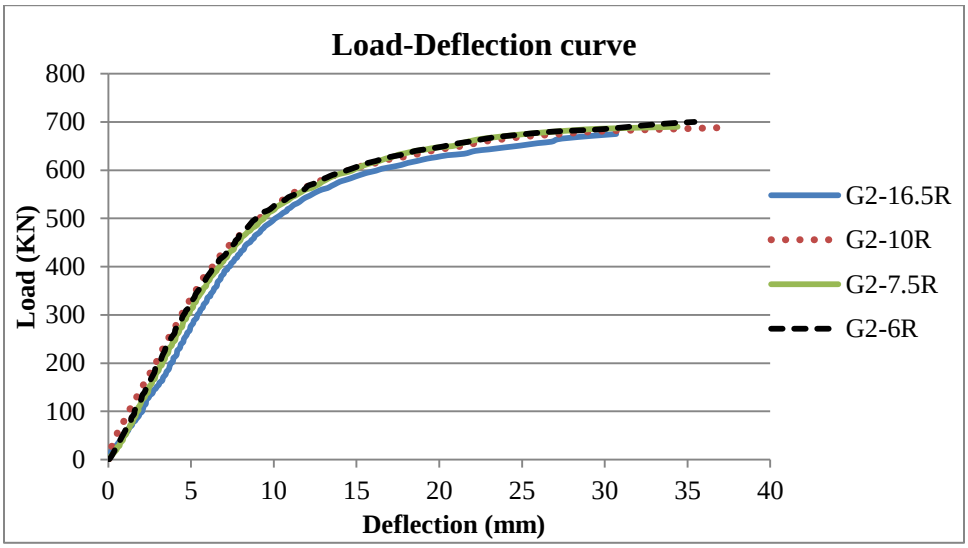

Figure 5.1 Load-deflection curves of girders

Table 5.1 Summary of experiment results

Girder / Property	G2-16.5R	G2-10R	G2-7.5R	G2-6R
Shear connection level at negative moment region (%)	66	110	146	183
Cracking load (KN)	284	291	300	306
Yielding load (KN)	339	345	356	359
Ultimate load (KN)	675	688	695	700
Max deflection (mm)	30.69	34.83	34.95	35.41
Toughness (KN.mm)	15442	18174	19846	20622
Failure mode	Crushing of concrete	Crushing of concrete	De-bonding of CFRP	De-bonding of CFRP

Figure 5.2 Deflected shape of G2-10R at ultimate load

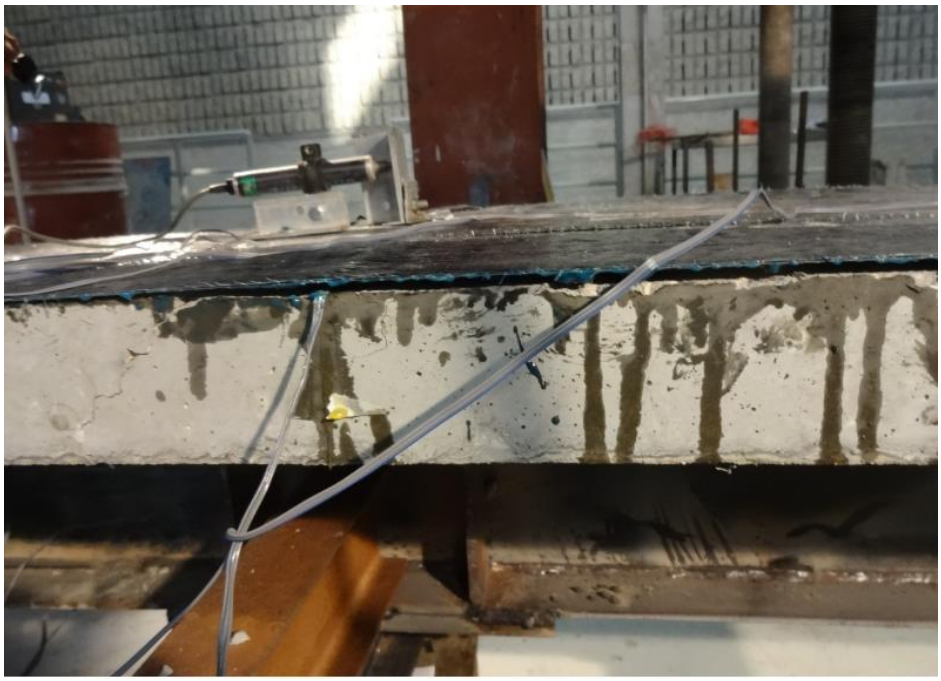

Figure 5.3 De-bonding of CFRP failure mode

5.2 Interface Slip and Strain Distribution

Interface slip developed during loading process at interior support is presented in Figure 5.4. It shows that the girders G2-10R, G2-7.5R, and G2-6R have almost same slip values at elastic stage. After that, the interface slip is affected by shear studs spacing at negative moment region. The increase of shear studs spacing leads to higher rate of slip and higher slip value at ultimate load. G2-16.5R starts slipping earlier with higher rate than other girders and achieves highest slip value at ultimate load (Table 5.2). Accordingly, the interface slip between concrete slab and steel beam at negative moment region is controlled by shear studs spacing. Girder G2-10R has reasonable slip value with respect to the designed slip value is obtained from push-out test (1.30mm). The partial composite action is not sufficient to prevent the interface slip.

Figure 5.5 shows load-slip curves at mid span for all girders. It is observed that the load-slip behavior is similar to the four girders. The slip values are varied within short range at different levels of loading (Table 5.2) where all girders have same shear studs spacing at positive moment region. Comparison between the interface slip at negative and positive moment regions shows that the slip values are higher at mid span for girders with full composite action at negative moment region. Girder G2-16.5R which has partial composite action slips more at negative moment region. It is influenced by shear studs spacing which is larger at negative moment region.

Table 5.2 Interface slip at different level of loading

Location	Load level	G2-16.5R	G2-10R	G2-7.5R	G2-6R
Slip at interior support (mm)	At cracking load	0.07	0.07	0.06	0.05
	At yielding load	0.16	0.11	0.10	0.07
	At ultimate load	1.90	1.37	0.51	0.34
Slip at mid-span (mm)	At cracking load	0.07	0.09	0.08	0.10
	At yielding load	0.11	0.13	0.12	0.13
	At ultimate load	1.36	1.39	1.45	1.41

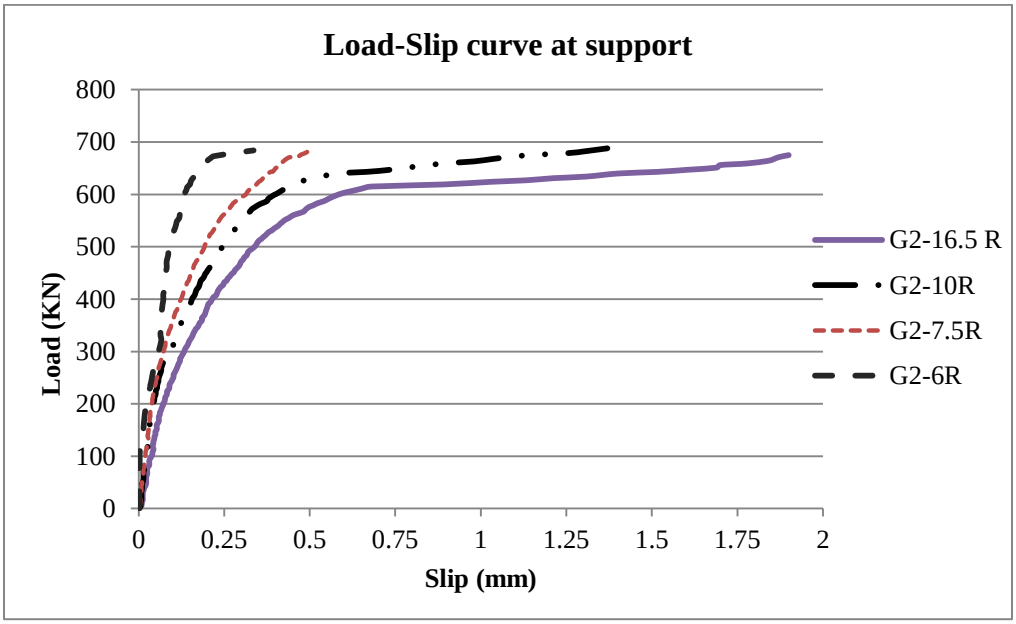

Figure 5.4 Load slip curve at the interior support

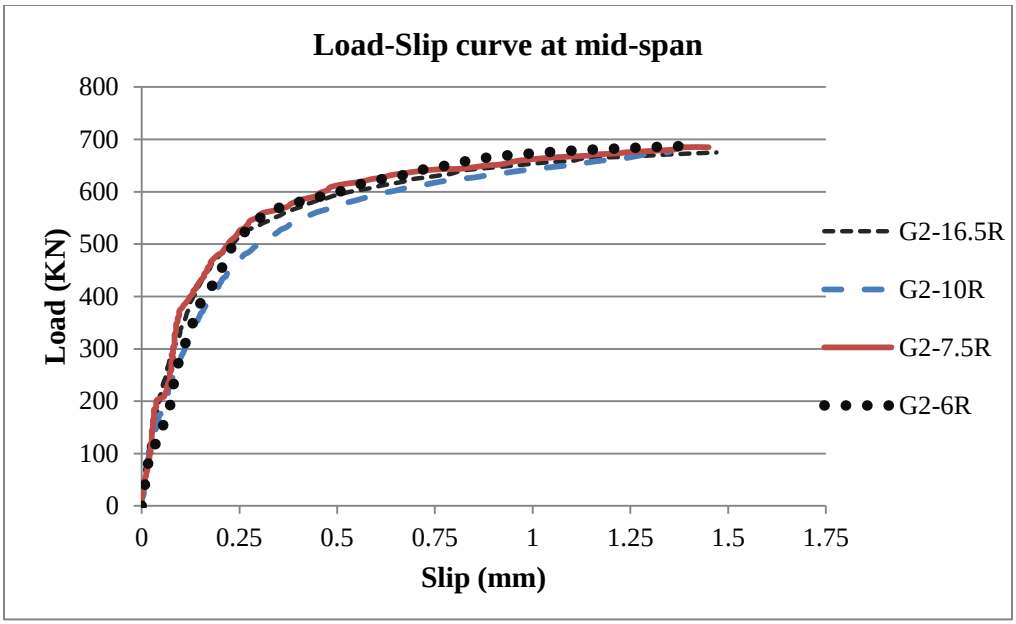

Figure 5.5 Load slip curve at mid-span

The strain development at interior support for the four girders is shown in Figure 5.6 through Figure 5.9. The strain is drawn at cracking load, yielding load, and at ultimate load, respectively. Comparison of the strain distribution between girders shows that the four girders have close strain values during elastic stage. Girders with full composite action have almost linear strain distribution along the cross section while G2-16.5R has different strain values at the interface between top flange and concrete slab. At ultimate load which represents the plastic stage, the nonlinearity in strain distribution becomes clear and the strain difference becomes larger. This gap between strain values is increased with increasing shear studs spacing which means more interface slip.

Figure 5.10 through Figure 5.13 show the development of strain values at the top flange and bottom of concrete slab during loading process. The difference between strain values represents the interface slip. It is noted that the interface slip is small at early stage of loading then it increases gradually with increasing the load. Girders with larger shear studs spacing exhibit larger strain difference which means higher slip value.

Girders G2-10R, G2-7.5R, and G2-6R achieve close strain values at ultimate load (about 9500με at bottom flange) while G2-16.5R attains less strain values (about 6900με at bottom flange). This is presumably because at ultimate load, the full composite girders deflect more than partial composite girder.

As a conclusion, shear studs play an important role in preventing interface slip between steel beam and concrete slab. 100% of full composite action is sufficient to keep slip values within acceptable range. Partial composite design is not recommended when structure is sensitive to the slip. The increase of composite action beyond 100% has negligible effect on the ultimate strain values.

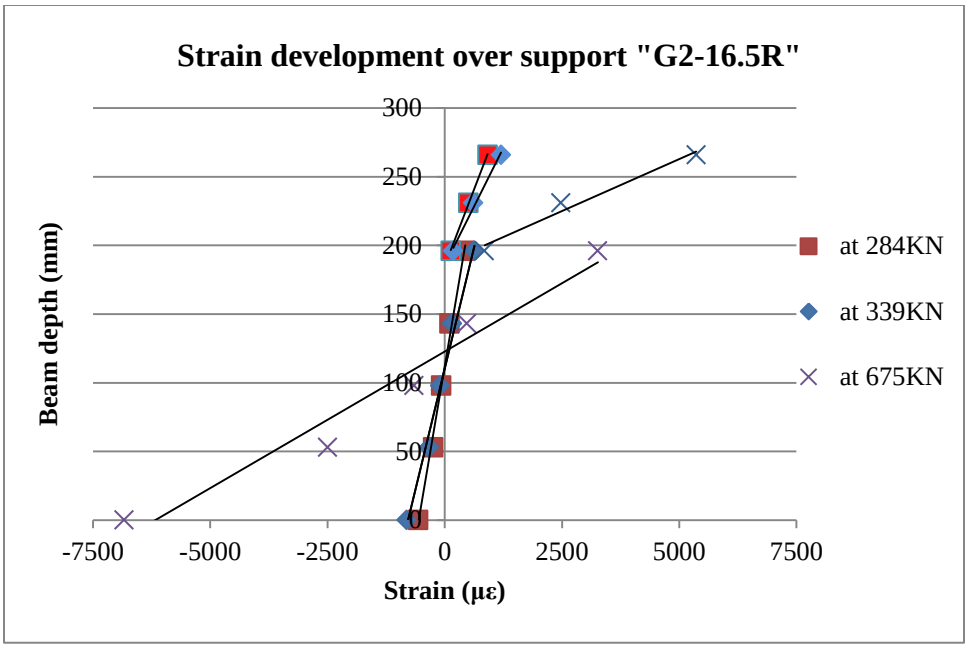

Figure 5.6 Cross-sectional strain distribution at interior support of G2-16.5R

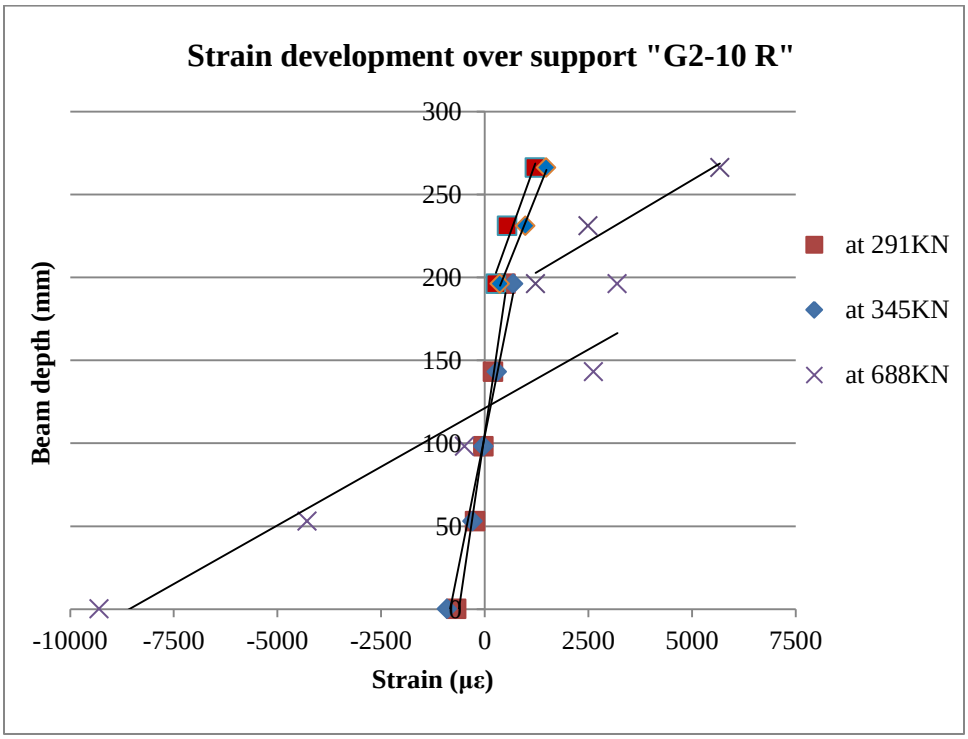

Figure 5.7 Cross-sectional strain distribution at interior support of G2-10R

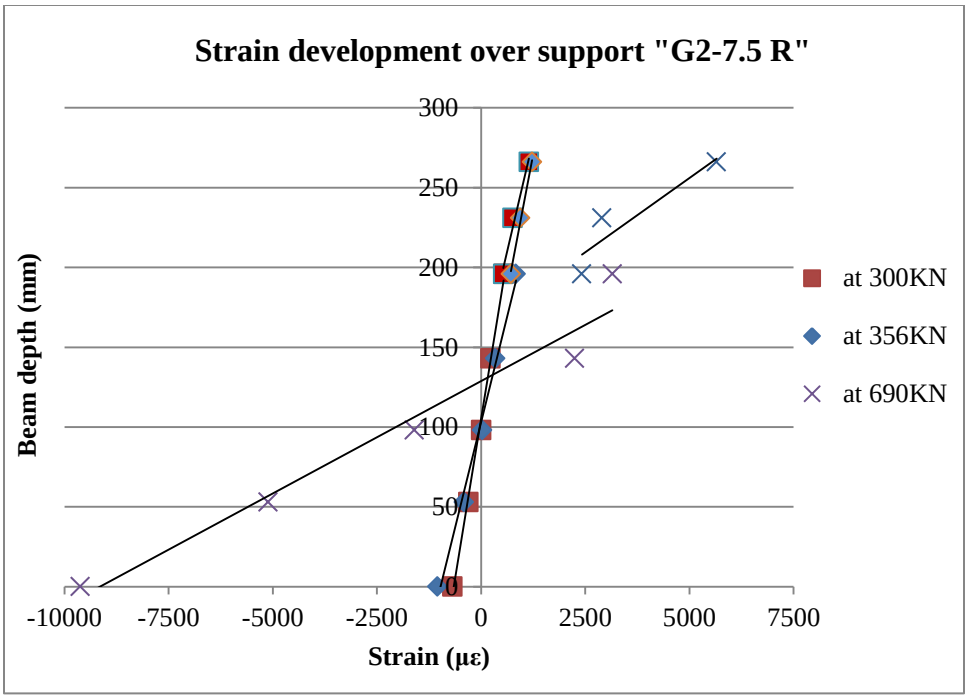

Figure 5.8 Cross-sectional strain distribution at interior support of G2-7.5R

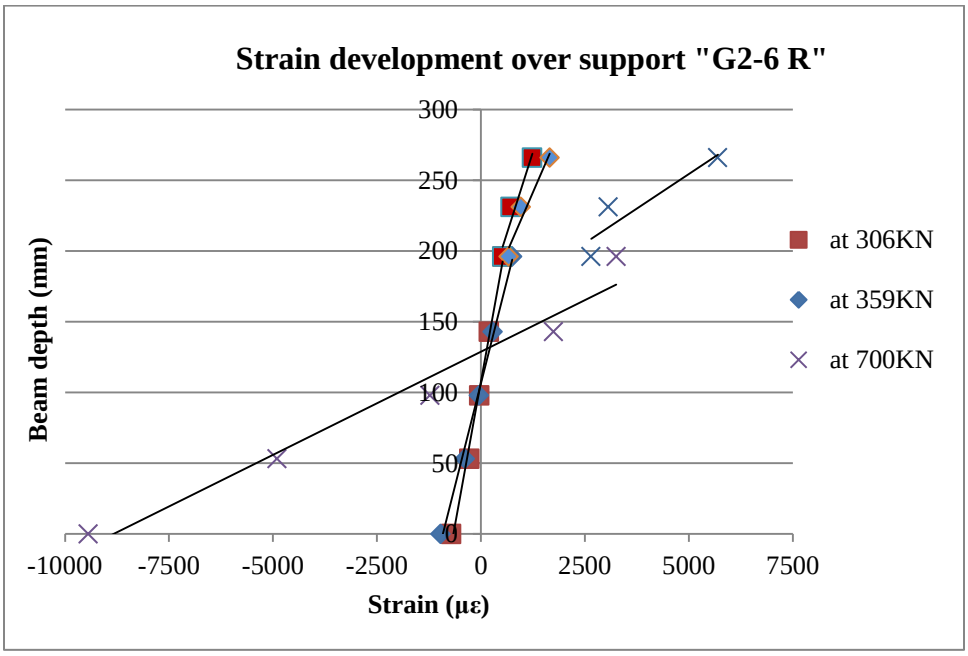

Figure 5.9 Cross-sectional strain distribution at interior support of G2-6R

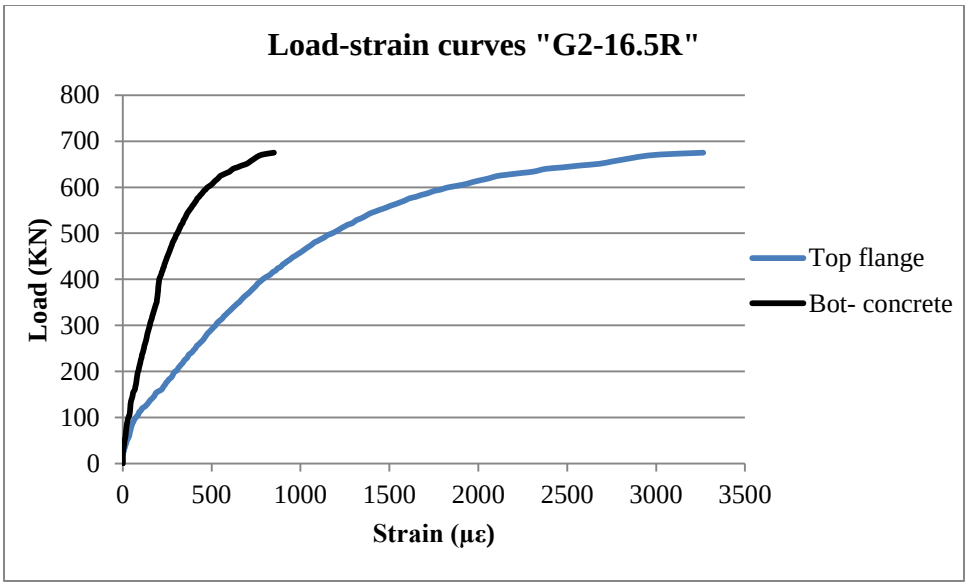

Figure 5.10 Load-strain curves of G2-16.5R

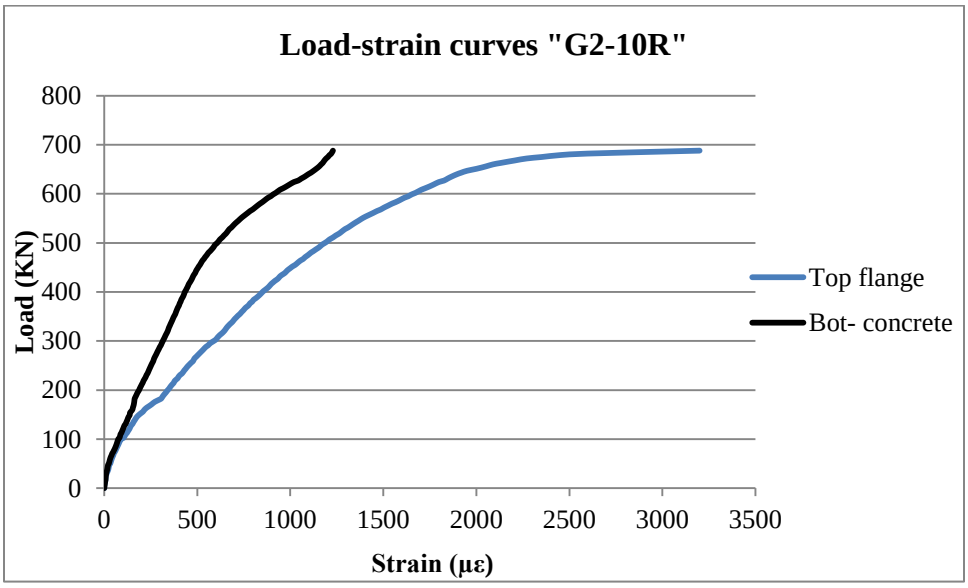

Figure 5.11 Load-strain curves of G2-10R

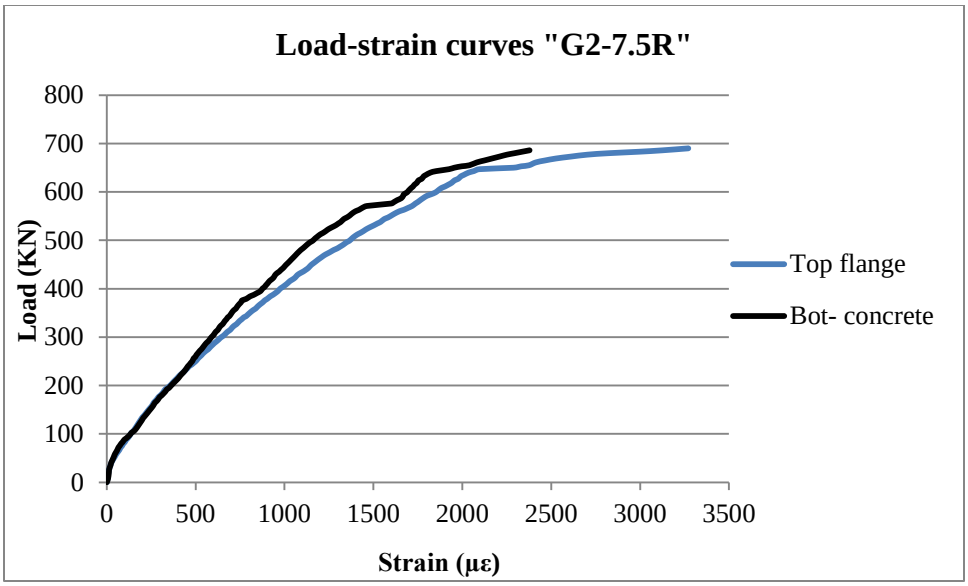

Figure 5.12 Load-strain curves of G2-7.5R

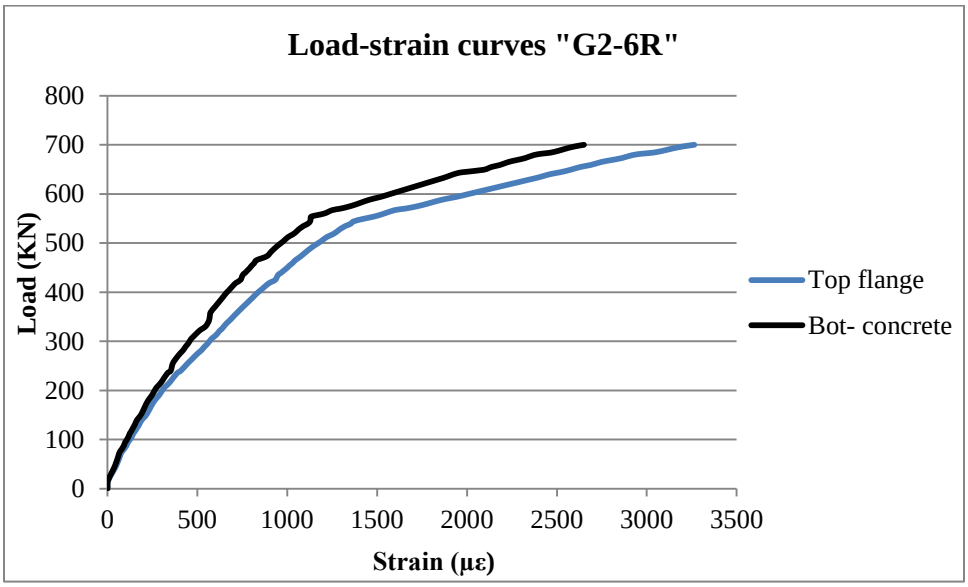

Figure 5.13 Load-strain curves of G2-6R

5.3 Load and Crack Development

Cracks concentrated at the interior support region mainly where the concrete slab are under tension. Although the top of concrete slab is covered with CFRP sheets, cracks distribution and propagation are observed at both edges of the concrete slab. The development of crack width is almost the same for all girders at elastic stage up to 500KN. After that, the crack width is controlled by shear studs spacing, it increases by the increase of shear studs spacing (Figure 5.14). The crack's width at ultimate load for G2-16.5R, G2-10R, G2-7.5, and G2-6R are 2.08, 1.48, 1.29, and 1.26 mm, respectively.

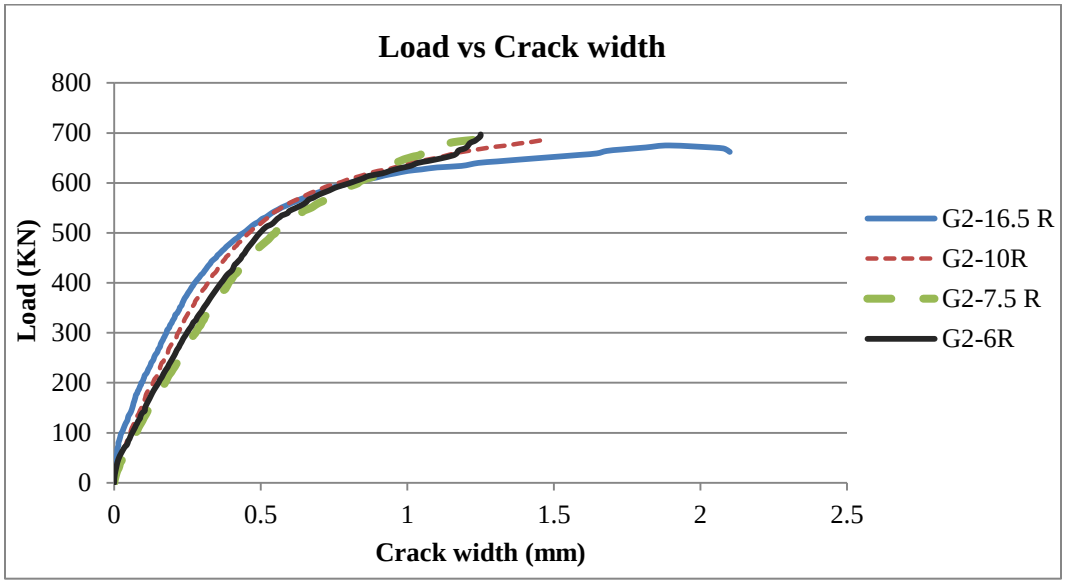

Figure 5.14 Crack width development

5.4 CFRP Performance

Two layers of CFRP were bonded to the top of concrete slab at negative moment region for maintaining the composite action. Six strain gauges were distributed over the top of CFRP layers to measure the strain development during the loading process. It was observed that the strain development is symmetric at both sides of the interior support with maximum value over the support. Moreover, the strain values for full composite girders (G2-10R, G2-7.5R, and G2-6R) are almost the same at elastic stage while G2-16.5R develops less strain value at same stage of loading (Figure 5.15). This is because the cracks are wider in full composite girders at elastic stage and the strain develops in CFRP is higher to resist the developed cracks. Whereas, cracks are smaller in G2-16.5R which causes lower strain in CFRP.

Shear connection level at negative moment region has slight effect on the CFRP strain at ultimate load. G2-16.5R and G2-10R achieve close strain value whereas G2-7.5R and G2-6R attain little bit higher strain in CFRP as shown in Figure 5.16. CFRP strain develops rapidly in G2-16.5R because the crack's width also increases rapidly at same interval of loading. Comparison between ultimate strain and failure modes shows that the girders are failed by crushing of concrete reach strain values close to de-bonding strain.

The shear stress at the interface between CFRP and concrete is calculated using analytical model proposed by Rosenboom & Rizkalla (2008) as the following,

$$\tau_w(x) = \frac{d}{dx}[K_p(x)\varepsilon_p(x)] \quad (5.1)$$

where $d/dx[\varepsilon_p(x)]$ is the change in CFRP strain along the beam length x, K_p is the axial stiffness of CFRP per unit width and equal to $n\ t_f\ E_f$. E_f is the elastic modulus of CFRP and $n\ t_f$ represents the thickness of CFRP configuration.

Results of G2-6R will be used to explain the calculation procedure as an example. The change in CFRP strain is the derivative of equation that represents the variation of longitudinal CFRP strain as shown in Figure 5.17.

$d/dx[\varepsilon_p(x)]$ at x=2000mm from the edge of girder.

$= 2.045x10^{-5}$.

$K_p = 0.5x230000$ (0.5mm is thickness of CFRP with epoxy)

$= 115000\ N/mm$

$\tau_w = 2.35\ N/mm^2$

Using same procedure, the shear stress for G2-16.5R, G2-10R, and G2-7.5R are 1.90, 1.79, 2.15 N/mm^2 respectively. These values explain the reason of de-bonding failure in G2-6R and G2-7.5R.

The relationship between CFRP strain and applied load is similar for full composite girders, while CFRP strain develops in slower rate in G2-16.5R (Figure 5.18). But eventually, all girders reach close strain values at ultimate load as discussed before. CFRP and concrete behave compositely during loading process where the strain values of CFRP and its corresponding point on concrete slab are very close. Figure 5.19 shows the development of CFRP and concrete strains for girder G2-10R as an example.

As a conclusion, G2-10R has proper shear studs spacing at negative moment region to get high performance for CFRP at elastic and plastic stages. In addition, full capacity of girder cross section can be exploited before reaching de-bonding strain in CFRP.

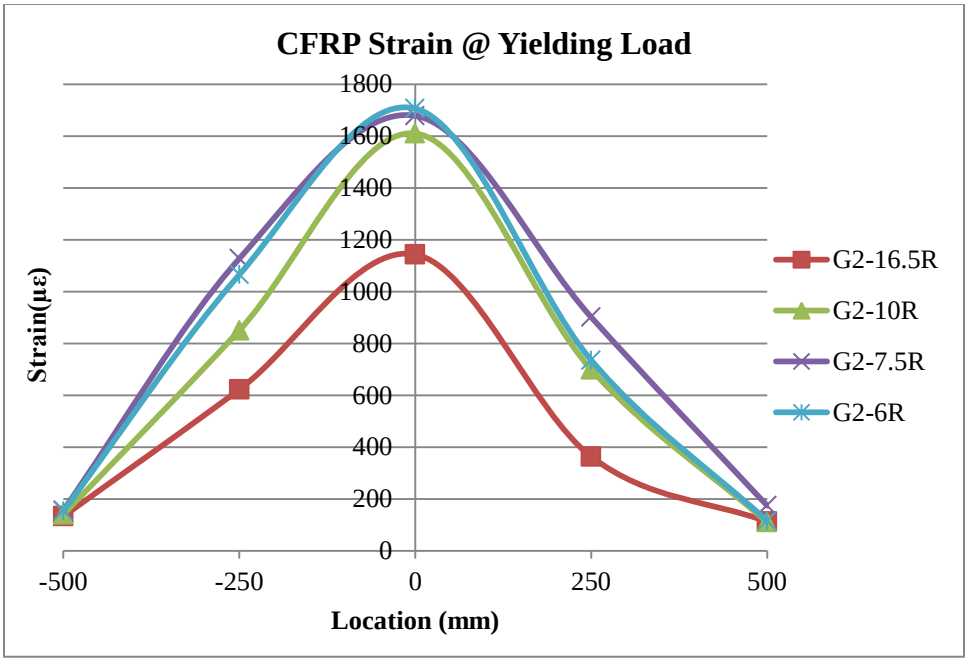

Figure 5.15 CFRP strain distribution at yielding load

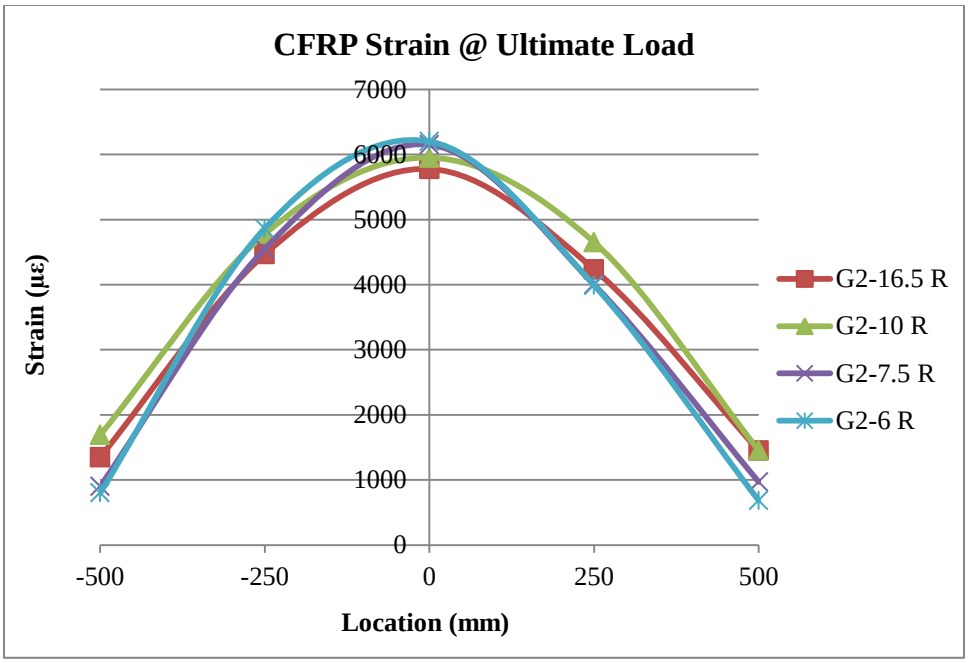

Figure 5.16 CFRP strain distribution at ultimate load

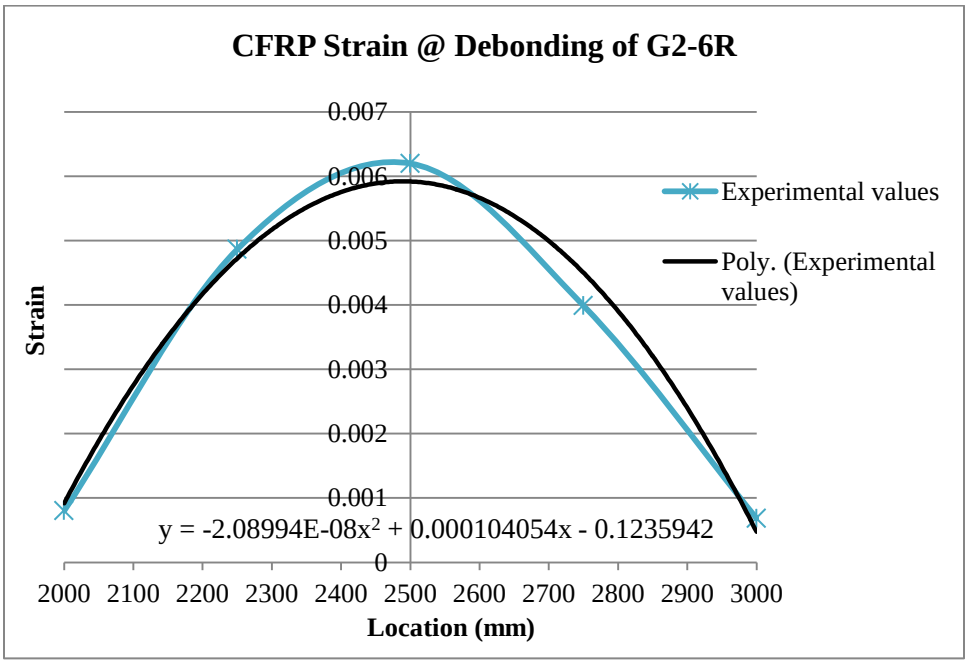

Figure 5.17 Variation of CFRP strain of G2-6R at de-bonding

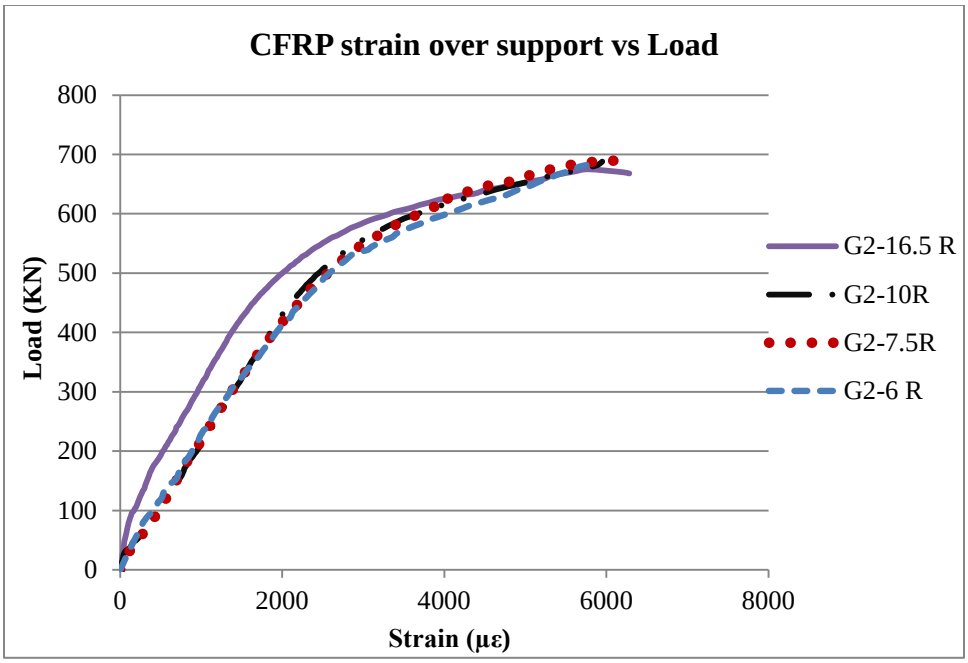

Figure 5.18 CFRP strain development during loading process

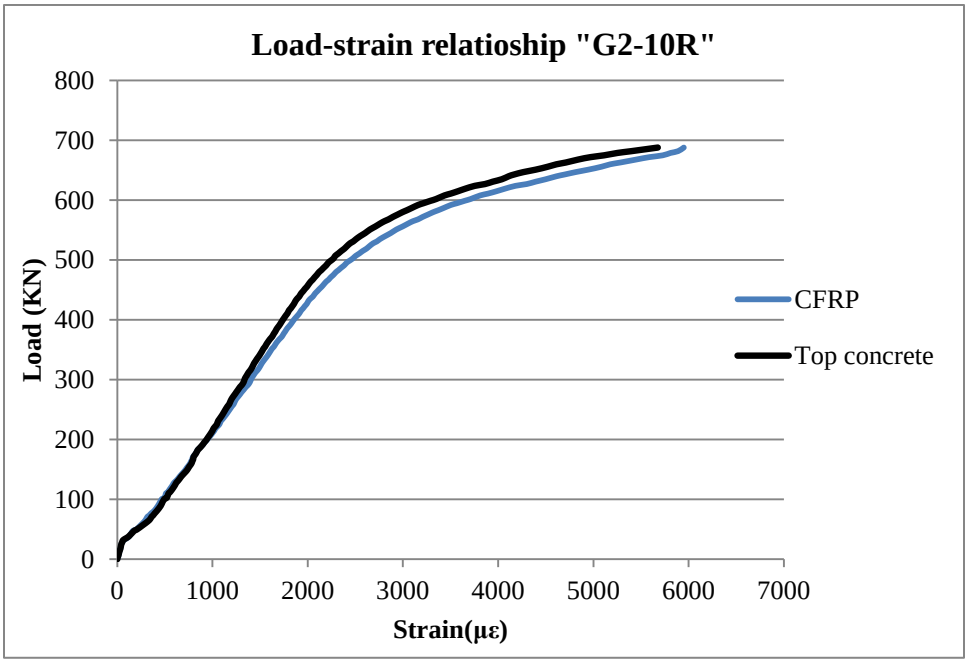

Figure 5.19 Comparison between CFRP and concrete strain at interior support

CHAPTER 6

FINITE ELEMENT ANALYSIS

6.1 General

Finite element studies and their comparison with experimental results are becoming very important to understand the real behavior of actual specimens. In recent years many researches and studies have been conducted on the composite girders using different finite element software.

ABAQUS 6.13 software was used to create 3D nonlinear finite element models for the tested girders in addition to nine girders with variable shear studs spacing at negative moment region and full composite action at positive moment region. These nine girders represent parametric study to evaluate the effects of shear studs spacing on the load-deflection behavior, interface slip, and CFRP strain. The simulation was conducted by means of dynamic explicit analysis. This method is very efficient in nonlinear problems containing material damage, large deformation, and complicated interactions. Finite element outcomes were verified with experimental results. The behavior of continuous composite girders was investigated with different shear studs spacing at negative moment region and presence of CFRP sheets bonded to the top of concrete slab. Interface slip

between concrete slab and steel beam, cracks distribution, load capacity and deflection, and CFRP stress were analyzed and compared with experimental results.

6.2 Girders Geometry and Mesh

Full scale composite girders were modeled using ABAQUS/Explicit. Each component of the composite girders was created as a separate part, then parts were assembled together to form a complete composite girder.

The steel beam, stiffeners, support plates, shear studs, and concrete slab were modeled using 3D stress 8-node linear brick element (C3D8R). The brick elements give accurate solution, good rate of convergence, and reduce analysis time. CFRP was modeled using 4-node doubly curved thin or thick shell element (S4R). This type of elements is useful for thin-walled structures which undergo large nonlinear deformation. The use of shell elements gives a good rate of convergence and reduces analysis time. Steel reinforcement was modeled using 2-node linear 3-D truss element (T3D2), Hibbitt (2013). Figure 6.1 shows the geometry of modeled girder.

Various model components were meshed part by part and moderate mesh size was used. Hex element shape with structured and sweep techniques were used to generate regular elements shape. Figure 6.2 displays the modeled girder after meshing.

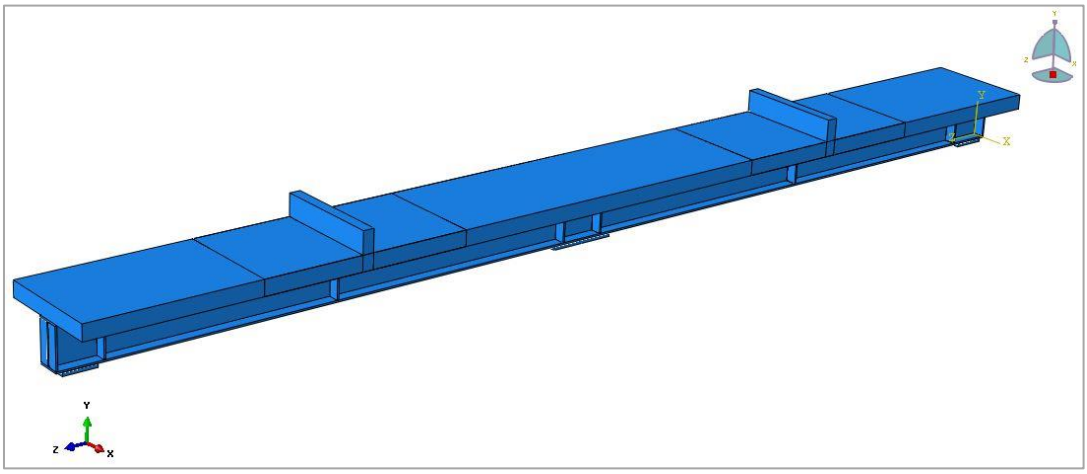

Figure 6.1 The geometry of the assembled modeled girder

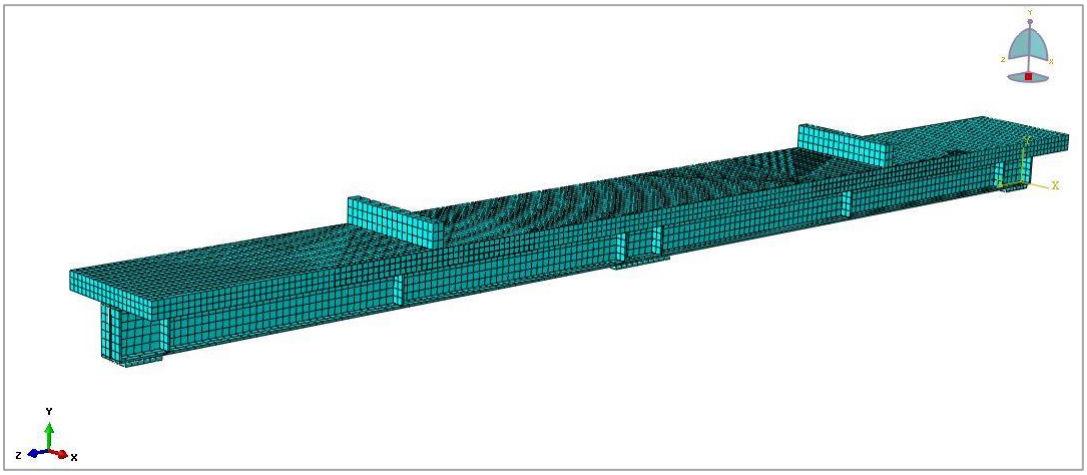

Figure 6.2 Overview of the meshed model

6.3 Boundary Conditions and Load

Steel plates were created at supports regions. Roller support system was simulated by cross line at the mid of the support plate and the movement was restrained in two directions (x, y). For pin and lateral support system, cross line was also defined at the mid of support plate and the movement was restrained in all three directions. For applying load purpose, steel plate was created at the mid of each span over the full width of concrete slab.

Girders were analyzed using displacement control; uniform displacement was applied to the top of loading plate. The total force was calculated by summing up the reaction on the supports plates nodes.

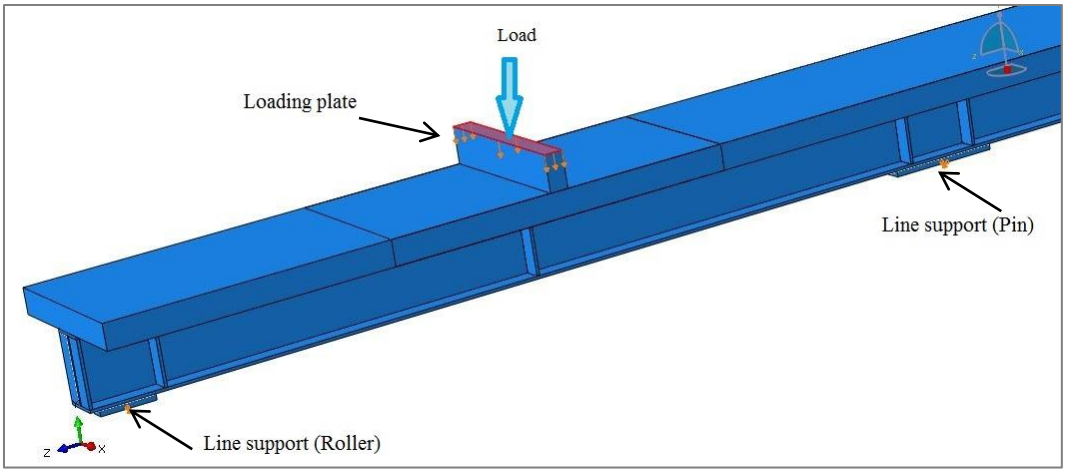

Figure 6.3 Boundary conditions of the modeled girders

6.4 Contact Interactions and Constraints

When all parts of the girder model were assembled together, appropriate contact were defined between different parts. The tie constraint was used to model welded regions like stiffener to steel beam, supports plates to the bottom flange, and shear studs to the top flange. It was also used between loading plates and concrete slab. Mechanical contact property was used to model the interaction between shear studs and concrete. Penalty friction formulation was used in tangential direction with coefficient of friction as 0.5. For normal direction, linear contact option was used. Shear studs surfaces were modeled as master and concrete surface around studs as slave. Steel reinforcement in both directions was defined as embedded region inside the concrete.

Cohesive contact property was used to simulate the adhesive material between the concrete and CFRP, the values of normal and tangential stiffness (K_{tt}, K_{ss}) were taken as 4000MPa. This value equals the slope of linear part of the relationship between shear stress/length vs. slip for adhesive material (Figure 6.4) Ziraba et al. (1994).

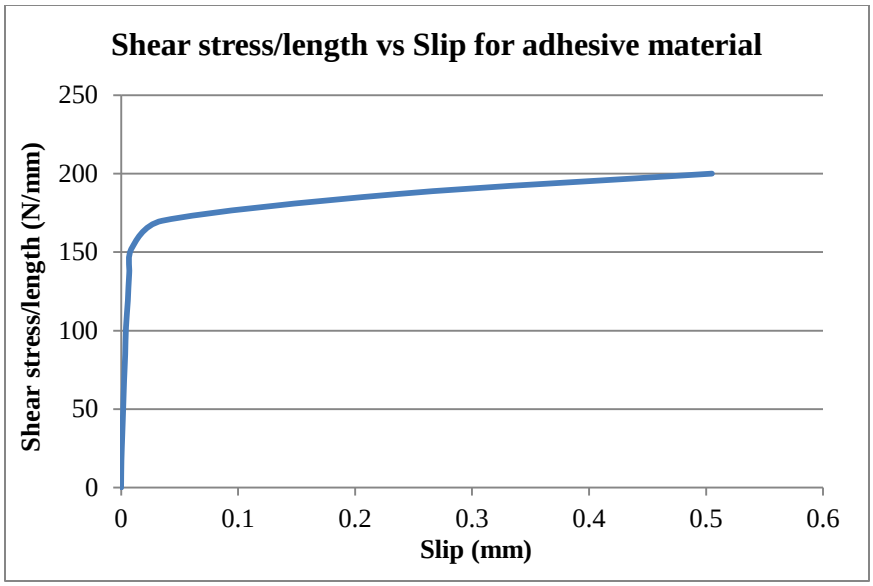

Figure 6.4 Shear stress/length vs. slip for adhesive material

6.5 Material Models

Concrete material properties were defined using concrete damage plasticity model (CDP). The failure mechanism was controlled by tensile cracking and compressive crushing of concrete. The concrete was modeled with an initial elastic material up to 35% of its compressive strength. Elastic modulus of concrete, Poisson's ratio, and concrete density were used in defining the concrete material in elastic range (Table 6.1).The parameters of plastic damage were used as shown in Table 6.2. The compressive stress-strain behavior at plastic range was represented in term of inelastic yield stress vs. inelastic strain (Figure 6.5) while the tensile stress-strain behavior was represented in term of yield stress vs. cracking strain.

The uniaxial degradation variables were modeled as monotonically increasing functions of the equivalent plastic strain. The degradation variables can take values ranging from 0, (undamaged material), to 1, (fully damaged material). If E_0 is the undamaged elastic stiffness of the concrete, the stress-strain relation under uniaxial tension and compression loading is expressed as in Equation (6-1) Jankowiak & Łodygowski (2005).

$$\sigma_t = (1 - d_t)\, E_0\, (\varepsilon_t - (\tilde{\varepsilon}^{pl})_t) \tag{6-1-a}$$

$$\sigma_c = (1 - d_c)\, E_0\, (\varepsilon_c - (\tilde{\varepsilon}^{pl})_c) \tag{6-1-b}$$

Table 6.1 Material properties of concrete

Property	Value
Elastic modulus (GPa)	23.8
Poisson's ratio	0.199
Density (kg/m^3)	2450

Table 6.2 Plastic damage parameter of concrete

Dilation Angle ψ	Flow potential eccentricity ε	f_{bo}/f_{co}	The ratio of second stress invariant K	Viscosity parameter v
36	0.1	1.16	0.67	0

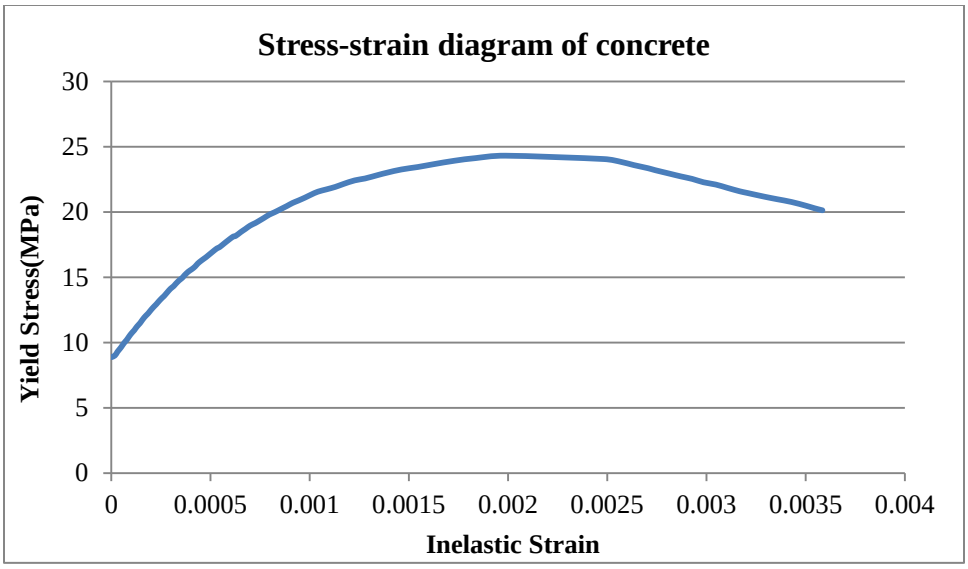

Figure 6.5 Stress-strain diagram of concrete at plastic range

The steel material; steel beam and reinforcement, and shear studs were defined as an elastic-plastic material. Elastic modulus of concrete, Poisson's ratio, and steel density were used in defining the steel materials in elastic range (Table 6.3). The stress-strain behavior of steel materials at plastic range was represented in term of inelastic yield stress vs. inelastic strain as shown in Figure 6.6.

Table 6.3 Material properties of steel

	Steel reinforcement	Steel plate
Elastic modulus (GPa)	205	202
Poisson's ratio	0.291	0.297
Density (kg/m^3)	7800	7800

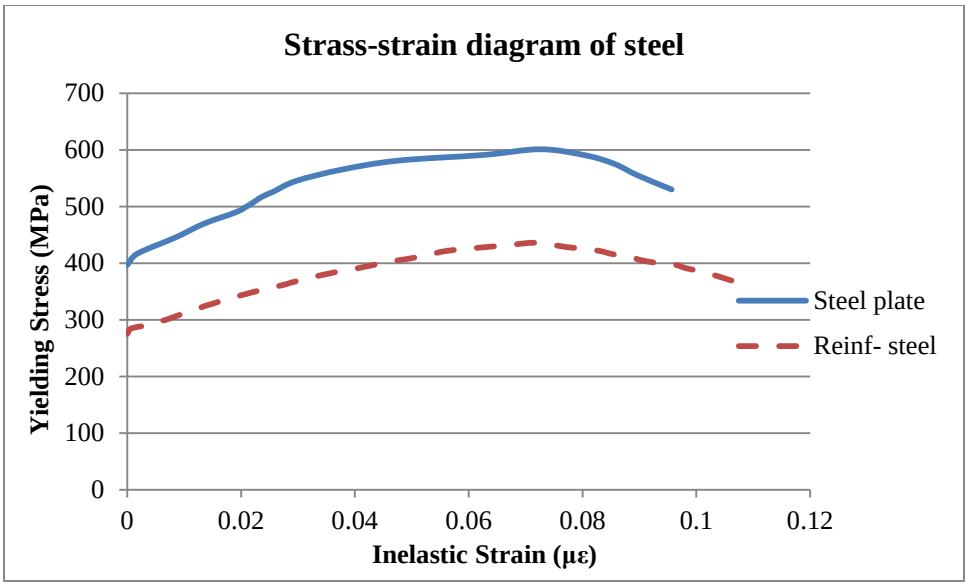

Figure 6.6 Stress-strain diagram of steel at plastic stage

CFRP was modeled as uni-directional laminate with thickness 0.131mm for each layer. CFRP was defined as linear elastic material. The properties were used in definition of CFRP presents in Table 6.4.

Table 6.4 CFRP Properties

Young modulus E1 (GPa)	Young modulus E2 (GPa)	Poisson's ratio u	Shear modulus G12 (MPa)	Shear modulus G13 (MPa)	Shear modulus G23 (MPa)	Ultimate stress σ_{ult} (MPa)
230	9	0.25	5000	50	50	1520

CHAPTER 7

FINITE ELEMENT RESULTS

This chapter presents the detailed results of finite element analysis for thirteen continuous composite girders. Four girders were modeled as that in the experimental work. The numerical results are validated and compared with the experimental data through load-deflection curves, interface slip, cracking of concrete slab, and CFRP stress. Another nine girders were modeled to study the performance of composite girders with variable shear studs spacing at negative moment region and CFRP bonded to the top of concrete slab. The behavior of composite girders is discussed through load-deflection curves, interface slip, and CFRP stress.

7.1 Validation of Finite Element Results

The finite element results are verified using experimental results as described in Chapter 5. Results of three girders (G2-16.5R, G2-10R, and G2-7.5R) are used to compare between experimental and numerical results. The comparison is made for the load-deflection curves and the interface slip for the three girders. Generally, the finite element results show good agreement with the experimental results. Figure 7.1 shows comparison between experimental and numerical load deflection curves for girder G2-16.5R. It is observed that the numerical curve exhibits slightly higher stiffness at elastic stage then it predicts more deflection than experimental curve at plastic stage. For girder G2-10R the

two curves are coincided at early stage of loading then the stiffness becomes slightly higher in the numerical analysis up to load value of 430KN. After that the numerical values predict more deflection than experimental results (Figure 7.2). Girder G2-7.5R exhibit higher stiffness numerically up to 500KN, then the two curves intersect and the numerical results predict more deflection with increasing the load as shown in Figure 7.3. The ultimate load capacity obtains experimentally is higher than numerical results within 2.5-3.5% for different girders while the numerical analysis predicts higher deflection with the difference ranging 9.5-13%. As a conclusion, all girders show higher stiffness at elastic stage numerically while the deflection becomes higher at plastic stage. The numerical analysis predicts lower ultimate load capacity with more deflection for different girders.

The validation of the modeling results is also carried out by comparing the interface slip between concrete slab and top flange of steel beam at the interior support. The numerical and experimental results show same load-slip behavior at elastic stage for girder G2-16.5R then the numerical slip values become higher up to ultimate load capacity (Figure 7.4). For girder G2-10R, the numerical slip values are lower than experimental slip up to 400KN. After that, the numerical analysis predicts higher slip till failure as shown in Figure 7.5. For girder G2-7.5R, the numerical slip is very small at early stage of loading and still less than experimental slip up to 450KN. The numerical and experimental slips values are very close together between 450-600KN, then the numerical slip become

larger up to failure (Figure 7.6). As a conclusion, all girders have similar load-slip performance where the numerical slip is lower than the experimental slip at elastic stage. Then it becomes higher during plastic stage up to failure load.

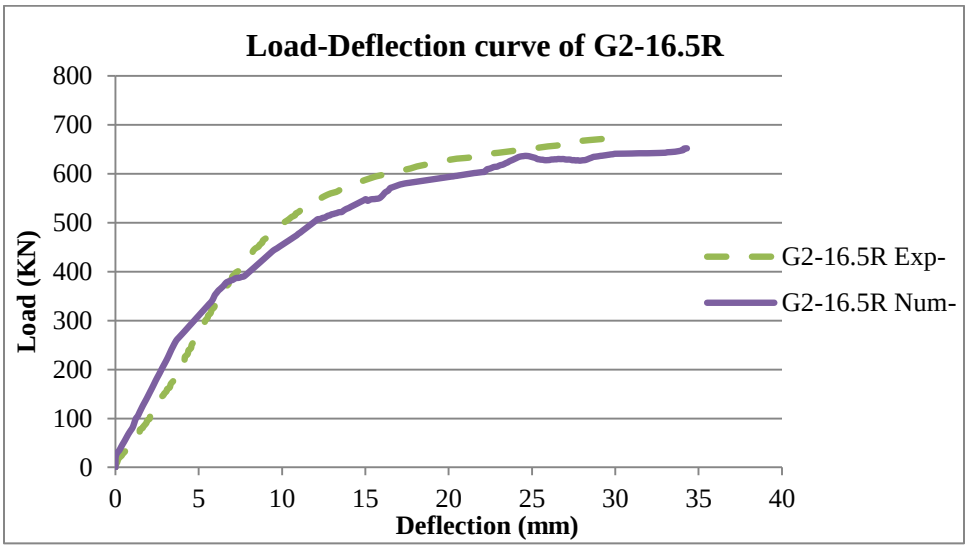

Figure 7.1 Load deflection curve of G2-16.5R

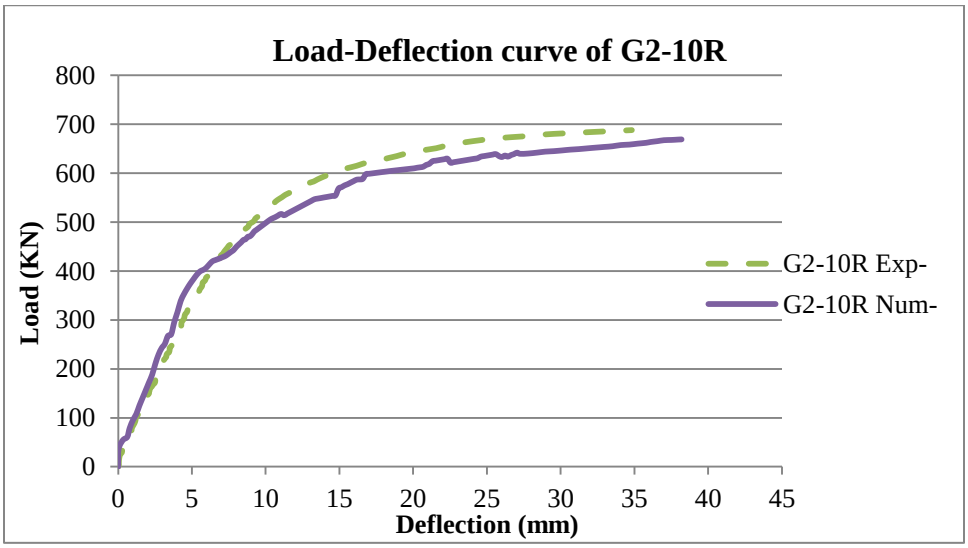

Figure 7.2 Load deflection curve of G2-10R

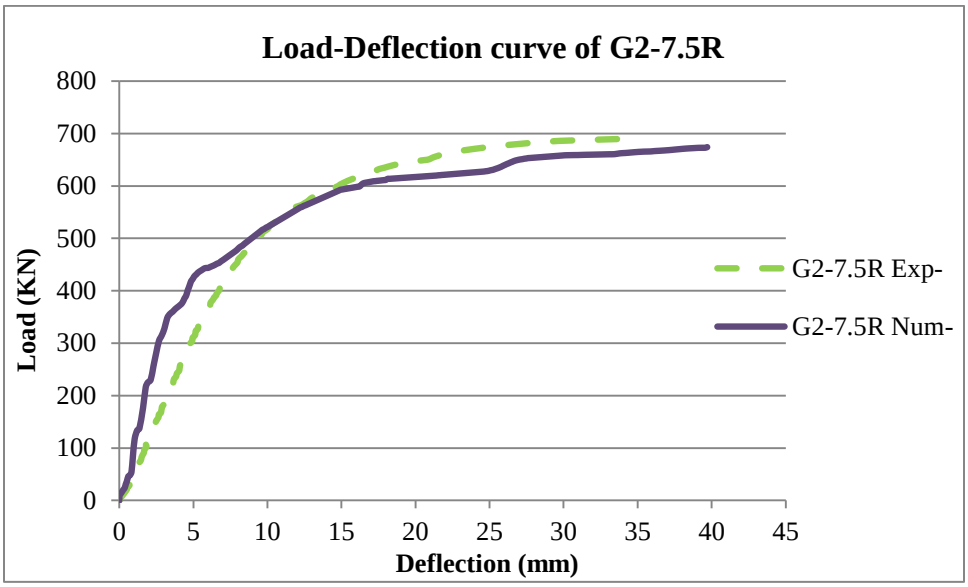

Figure 7.3 Load deflection curve of G2-7.5R

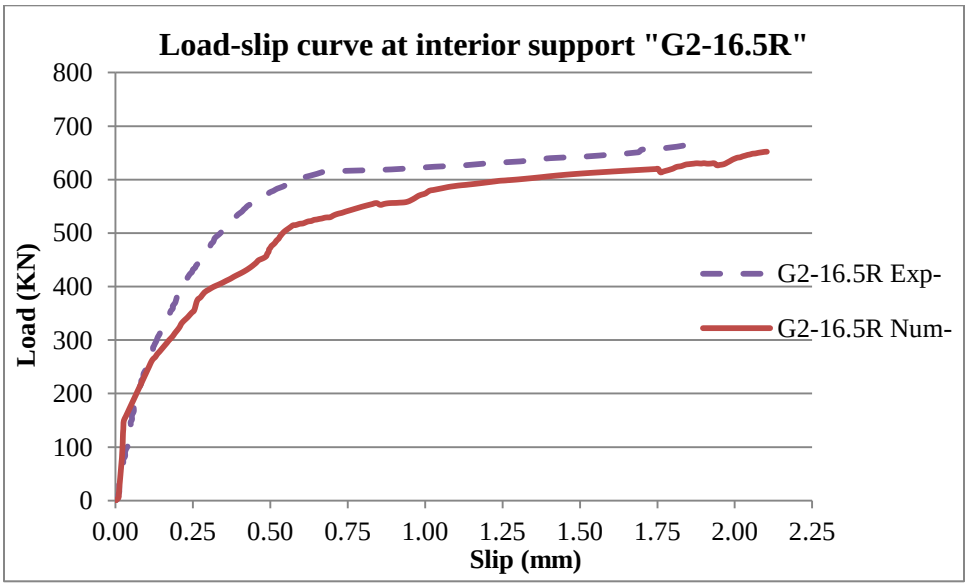

Figure 7.4 Load slip curves at interior support of G2-16.5R

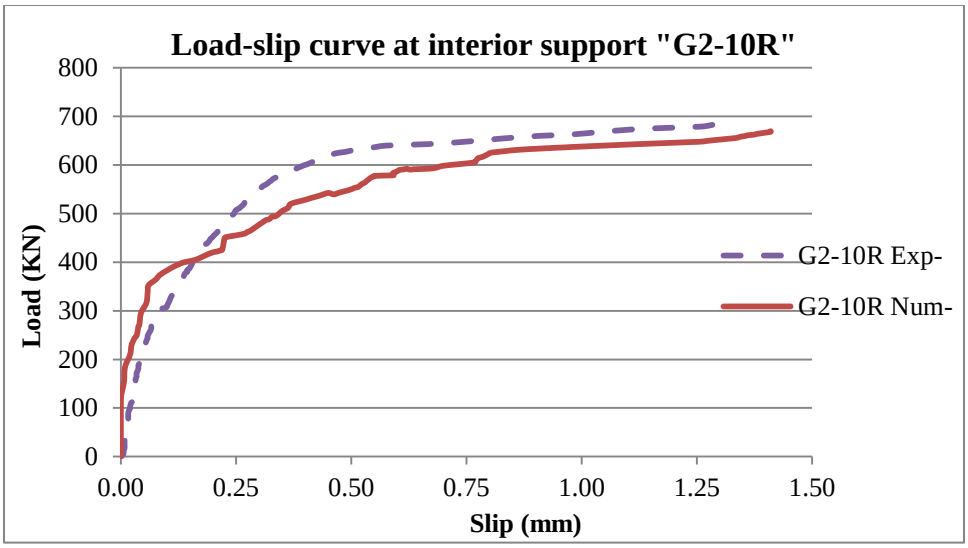

Figure 7.5 Load slip curves at interior support of G2-10R

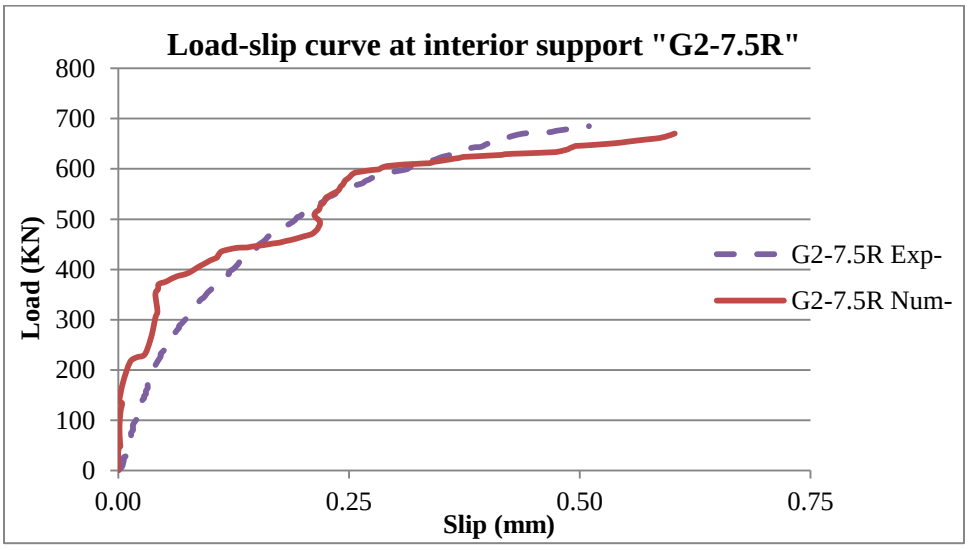

Figure 7.6 Load slip curves at interior support of G2-7.5R

7.2 Load and Deflection Curves

In the previous section numerical load-deflection curves are validated with experimental results and show good agreement. Figure 7.2 describes the load-deflection curves of all modeled girders. The girders stiffness increases with the increase of shear connection level at negative moment region at elastic stage up to 600KN. After that, the girders behavior closes together up to failure load. The finite element analysis predicts lower yielding and ultimate loads but higher deflection than values obtained in experimental work (Table 7.1). Figure 7.8 shows the deflected shape of G2-10R model.

Toughness is also calculated to compare between numerical and experimental results. The toughness values which are calculated from numerical curves are slightly higher than experimental values. This is because numerically the girders deflect more and the area under the load-deflection curve becomes larger.

The failure modes are the same for numerical and experimental, G2-6R and G2-7.5R are failed by de-bonding of CFRP whereas G2-16.5R and G2-10R are failed by crushing of concrete (Figure 7.9). As a conclusion, finite element analysis can be used to predict the general behavior of composite girder with lower stiffness at elastic stage. Ultimate load capacity can be predicted conservatively with excessive deflection.

Table 7.1 Comparison between numerical and experimental results

Property \ Girder		G2-16.5R	G2-10R	G2-7.5R	G2-6R
Yielding Load (KN)	Numerical	330	339	350	354
	Experiment	339	345	356	359
Ultimate Load (KN)	Numerical	652	669	674	682
	Experiment	675	688	695	700
Max Deflection (mm)	Numerical	34.30	38.20	39.70	40.30
	Experiment	30.69	34.83	34.95	35.41
Toughness (KN.mm)	Numerical	16832	20581	22387	23037
	Experiment	15442	18174	19846	20622
Failure Mode	Numerical	Crushing of concrete	Crushing of concrete	De-bonding of CFRP	De-bonding of CFRP
	Experiment				

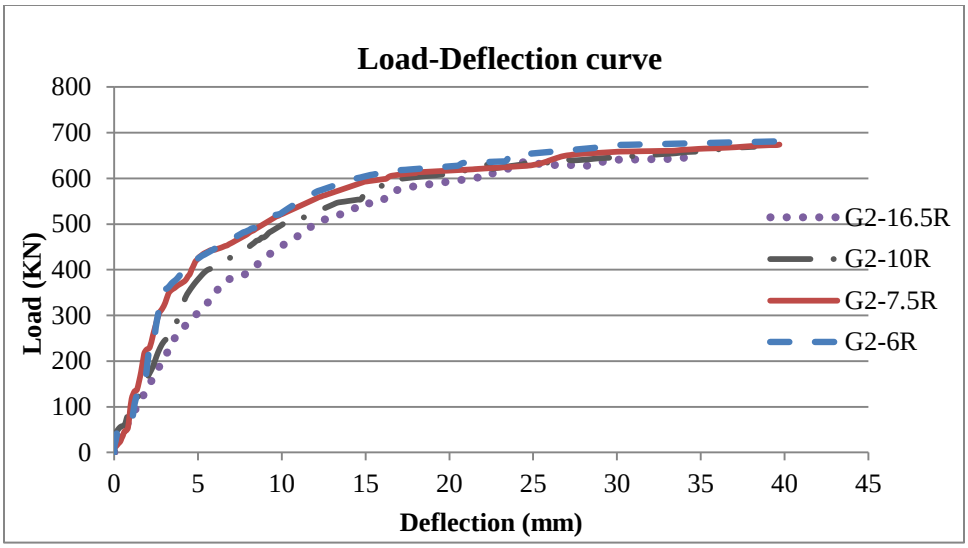

Figure 7.7 Load deflection curves of modeled girders

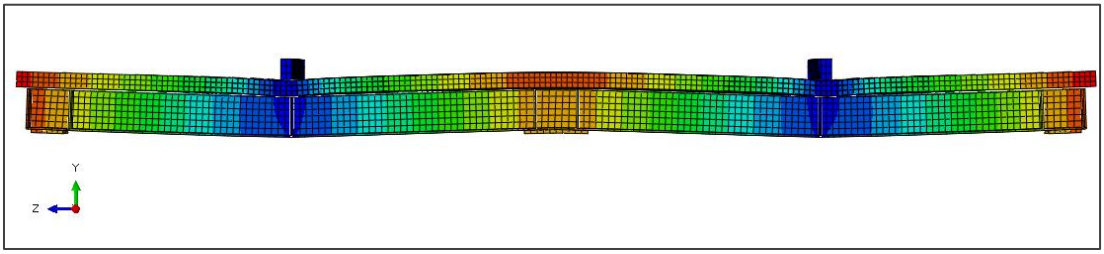

Figure 7.8 Deflected shape of G2-10R

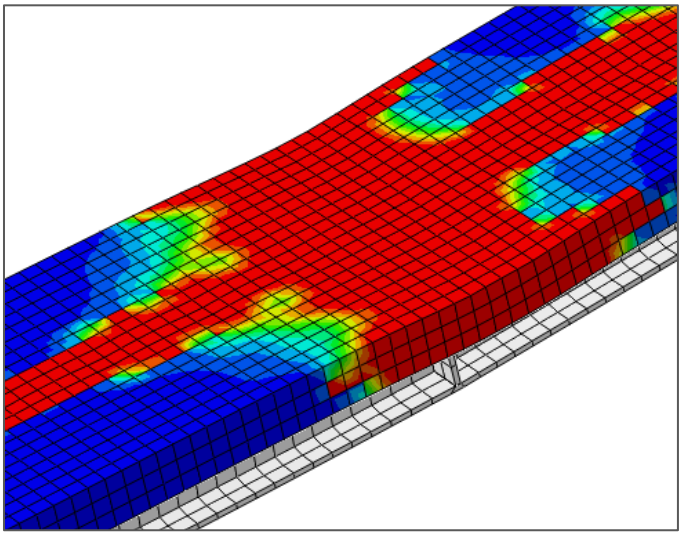

Figure 7.9 Crushing of concrete at mid-span

7.3 Interface Slip

The interface slip between top flange of steel beam and bottom of concrete slab during loading process at interior support is shown in Figure 7.10. It is measured as the difference in the horizontal displacement between two adjacent nodes in top flange and concrete slab. It is noted that the slip is very small at the early stages of loading then develops rapidly up to failure load. The finite element slip values at ultimate load are higher than experimental values (Table 7.2). This is presumably because the mid-span deflection is higher in the finite element analysis. The increase of shear studs spacing causes higher rate of slip and higher slip values at ultimate load.

Figure 7.11 shows the load-slip curves at mid-span. All modeled girders have similar load slip behavior and close slip values at ultimate load because all girders are modeled with same shear studs spacing at positive moment region. As noted at the interior support region, numerical slip values are higher than experimental values (Table 7.2). In addition, the slip at mid-span is higher than the slip at the interior support region. As a result, finite element analysis predicts higher values for the interface slip at positive and negative moment region.

Table 7.2 Comparison between slip values at ultimate load

Location		G2-16.5R	G2-10R	G2-7.5R	G2-6R
Slip at interior support(mm)	Numerical	2.10	1.41	0.6	0.52
	Experiment	1.90	1.37	0.51	0.34
Slip at mid-span(mm)	Numerical	1.39	1.46	1.50	1.52
	Experiment	1.36	1.39	1.45	1.41

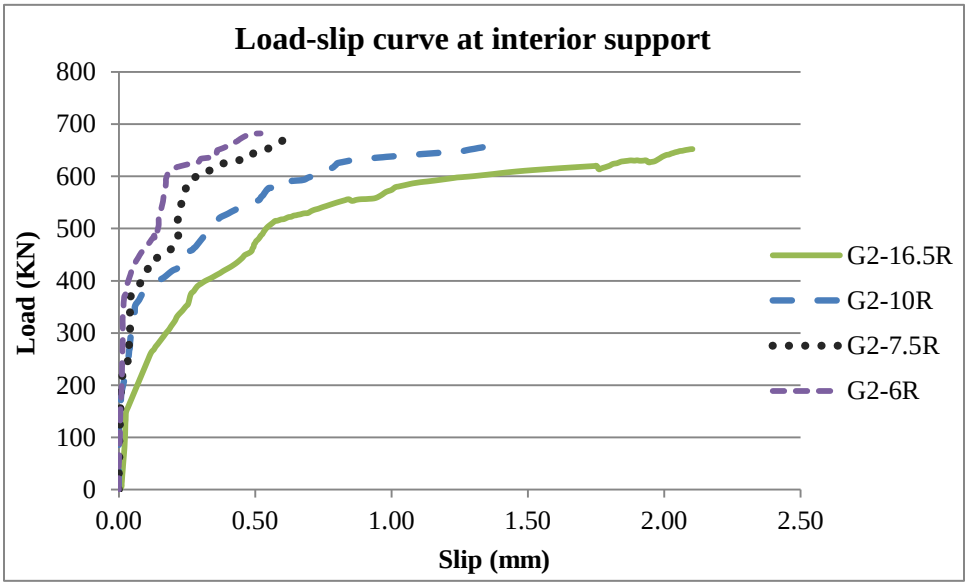

Figure 7.10 Load slip curves at interior support for modeled girders

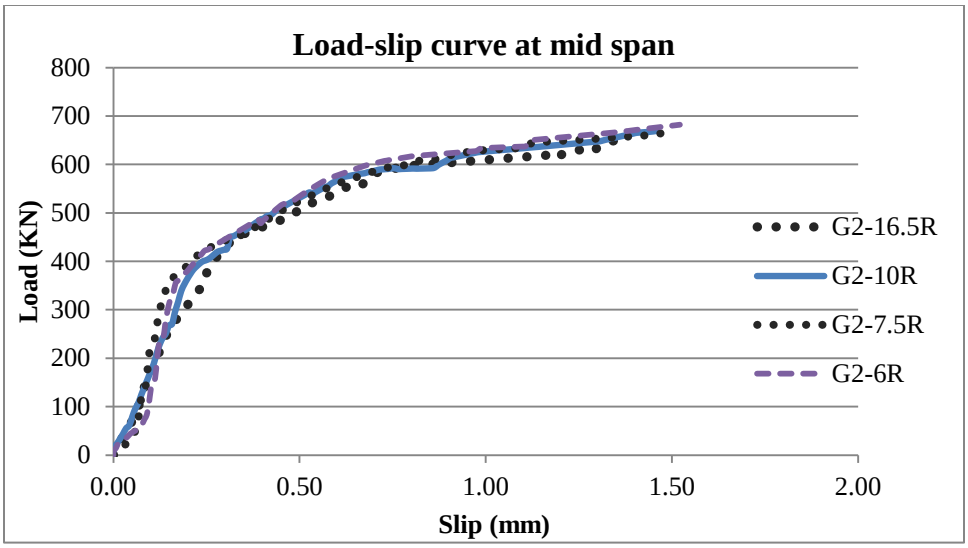

Figure 7.11 Load slip curves at mid-span for modeled girders

7.4 Cracking of Concrete

The damage plasticity model in ABAQUS is used to simulate the cracks distribution and propagation in the concrete slab. Figure 7.12 and Figure 7.13 present the crack distribution at the top of concrete slab at negative moment region for G2-6R and G2-16.5R, respectively. Some cracks are propagated over the entire slab width and thickness. The cracks at slab edges were also observed during testing of girders. The damage developed in G2-16.5R is more than that of G2-6R. This can be imitated with the crack width results in experimental work whereas the concrete damage increases with the increase of crack width. Therefore, the concrete damage at negative moment region increases with increasing the shear studs spacing. As a conclusion, plastic damage model is suitable to model cracks development in the concrete.

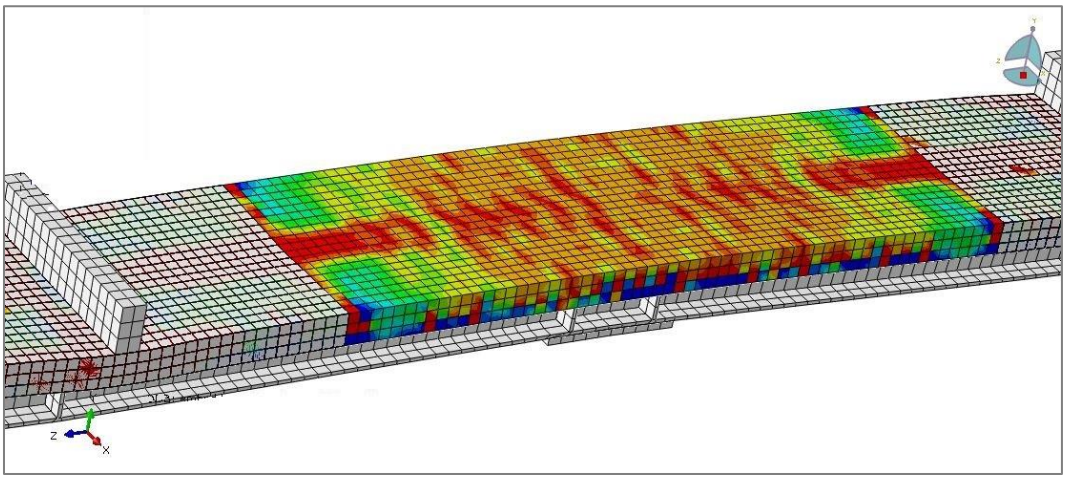

Figure 7.12 Concrete damage at negative moment region of G2-6R

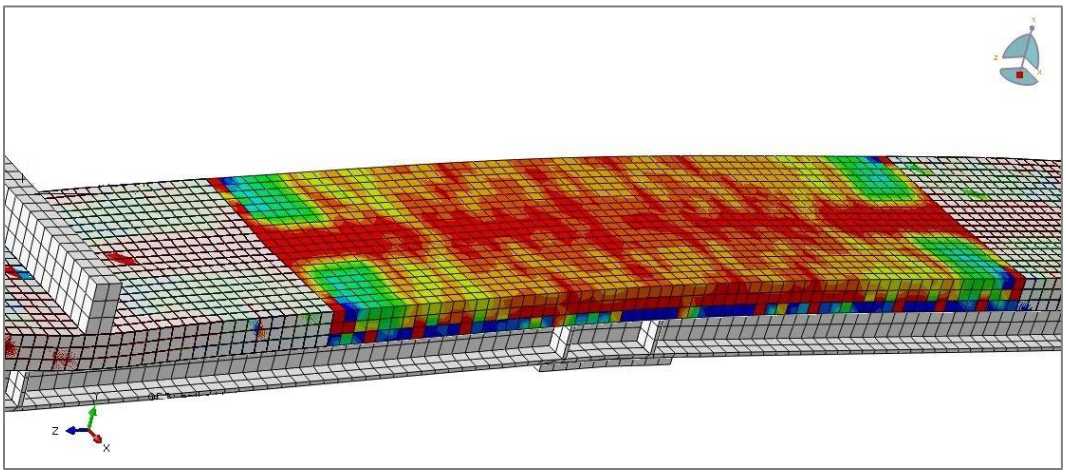

Figure 7.13 Concrete damage at negative moment region of G2-16.5R

7.5 CFRP Performance

In the modeled girders, CFRP sheets are bonded to the top of concrete slab at negative moment region with same dimension used in the tested girders. The strain develops in CFRP at negative moment region distribute symmetrically at both sides of the interior support is similar to the experimental results. Comparison between strains develops in CFRP shows that the finite element analysis predicts lower strain values at yielding load (Table 7.3). However, the numerical strain values at ultimate load exceed that achieved in the experimental work because the girders developed higher deflection values by the finite element analysis. The strain develops in CFRP at ultimate load is slightly varied according to shear connection level. Figure 7.14 shows the distribution of strain in CFRP at negative moment region for G2-10R as an example. It presents the symmetrical distribution and the maximum strain values at the center of CFRP sheet.

The shear stress at the interface between CFRP and concrete slab is calculated using same procedure mentioned in Section 5.4. It shows that the shear stress in girders G2-6R and G2-7.5R exceeds the shear strength capacity of the epoxy. Therefore, the de-bonding of CFRP is occurred. It is noticed that the de-bonding occurs at higher strain values compared to the experimental results because the mechanism of de-bonding depends on the general behavior of CFRP strain. The other girders are failed by crushing of concrete at positive moment region. These girders reach CFRP strain values close to that causing de-bonding failure.

Table 7.3 Comparison between CFRP strain values at interior support

		G2-16.5R	G2-10R	G2-7.5R	G2-6R
CFRP Strain at Yielding Load (με)	Numerical	1094	1575	1605	1660
	Experiment	1143	1610	1678	1706
CFRP Strain at Ultimate Load (με)	Numerical	5980	6240	6511	6580
	Experiment	5777	5950	6150	6200

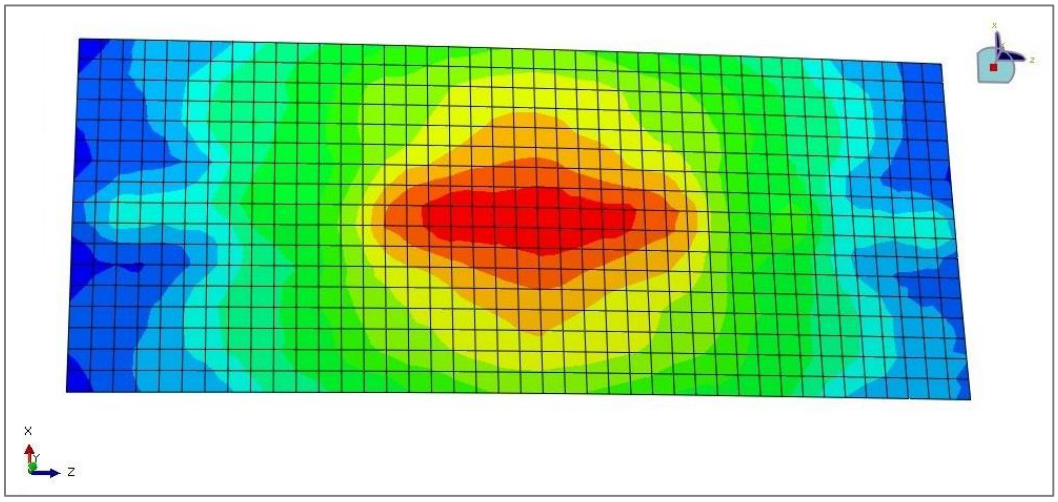

Figure 7.14 Stresses develop in CFRP of G2-10R

7.6 Parametric Study

In order to study the effect of shear studs spacing on ultimate load capacity, failure mode, interface slip, and CFRP strain, nine continuous composite girders were modeled with variable shear studs spacing at negative moment region (Table 7.4). The girders were modeled with dimensions, cross section, and bonded CFRP same that in the experimental work. Moreover, the shear studs spacing was determined to have full composite action at positive moment region (55mm shear studs spacing between inflection point and mid-span while 100mm shear studs spacing was used between mid-span and exterior support).

Table 7.4 Shear studs spacing at negative moment region

Girder	Shear studs spacing at negative moment region (mm)	Shear connection level (%)
G-18.3	183	60
G-15.7	157	70
G-13.8	138	80
G-12.2	122	90
G-11	110	100
G-10	100	110
G-9.2	92	120
G-8.5	85	130
G-7.8	78	140

7.6.1 Load and Deflection Curves

The results of the modeled girders are presented in Table 7.5. The results show that the yielding load and ultimate load values increase with the increase of shear connection level. Also, the flexibility of girders are controlled by shear studs spacing at negative moment region where the deflection at mid-span is increased with reducing shear studs spacing at negative moment region. All girders have close stiffness values at early stage of loading then it increases with the increase of shear connection level up to the failure (Figure 7.15).

Two failure modes are observed; crushing of concrete at mid-span and de-bonding of CFRP at negative moment region. The girders with smaller shear studs spacing failed by de-bonding of CFRP while increasing of shear studs spacing causing crushing of concrete failure. This is because the increase of shear studs number at negative moment region allows to develop higher stress value in CFRP, as will be discussed later, so the shear stress between CFRP and concrete increases causing de-bonding of CFRP.

As a conclusion, ultimate load capacity, mid-span deflection, and girder's stiffness are increased with reducing of shear studs spacing at negative moment region. Moreover, the shear studs spacing affects the failure mode where reducing shear studs spacing beyond full composite action causes de-bonding of CFRP failure mode.

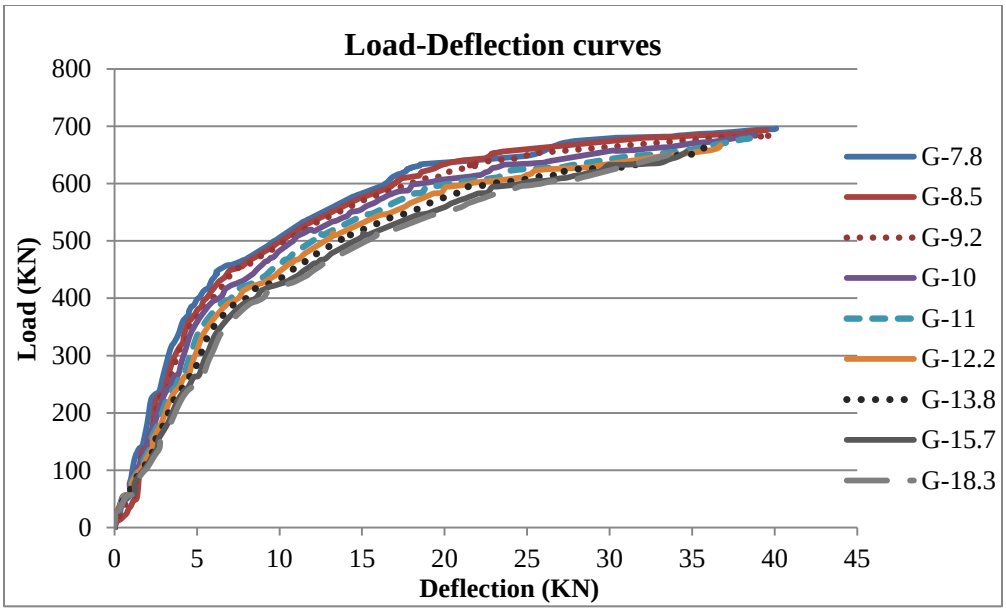

Figure 7.15 Load-deflection curves for parametric study girders

Table 7.5 Summary of parametric study results

Girder	Yielding Load (KN)	Ultimate Load (KN)	Deflection (mm)	Failure Mode
G-18.3	320	653	33.6	Crushing of Concrete
G-15.7	325	657	34.6	Crushing of Concrete
G-13.8	330	664	35.8	Crushing of Concrete
G-12.2	336	669	36.7	Crushing of Concrete
G-11	340	677	37.8	Crushing of Concrete
G-10	345	682	38.3	Crushing of Concrete
G-9.2	353	688	39.1	De-bonding of CFRP
G-8.5	359	693	39.5	De-bonding of CFRP
G-7.8	364	696	40.1	De-bonding of CFRP

7.6.2 Interface Slip

Figure 7.16 presents the development of interface slip during loading process at the interior support. It shows that the girders G-7.8, G-8.5, G-9.2, and G-10 have small slip values at elastic stage while girders G-11, G-12.2, G-13.8, G-15.7, and G-18.3 exhibit higher slip values at same stage of loading. The increase of shear studs spacing causes higher rate of slip and higher slip values at ultimate load where partial composite girders starts slipping earlier with higher rate than other girders and achieves higher slip values at ultimate load. Moreover, the slip values of partial composite girders at ultimate load exceed the design slip value (1.30mm). G-11 which represents 100% composite action at negative moment region achieves slip value (1.34mm) close to the design slip value. Figure 7.17 shows the relationship between shear connection level and interface slip at the interior support. It shows that the slip is decreased gradually with increasing of shear connection level.

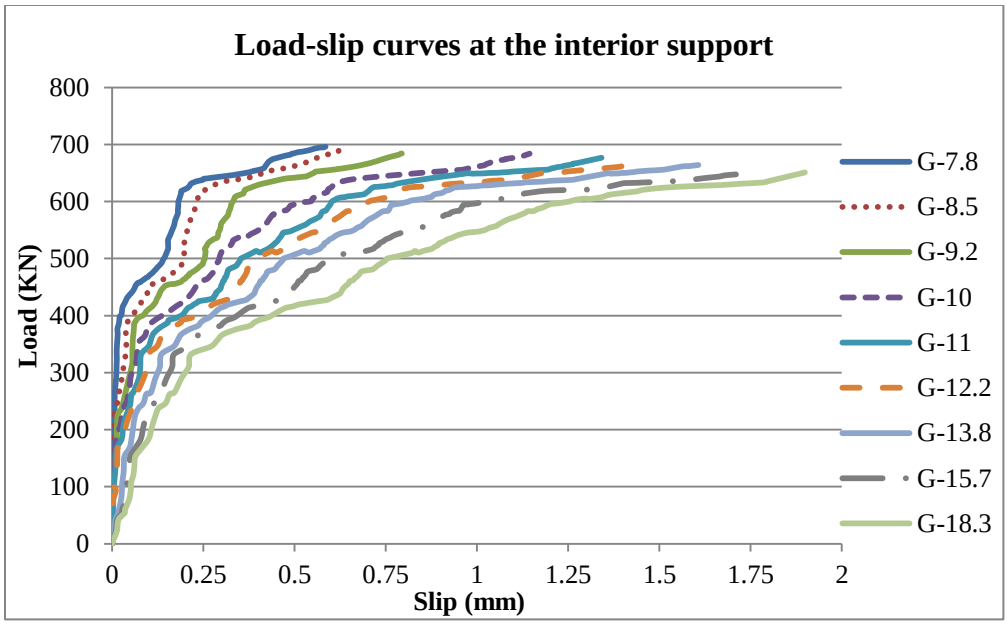

Figure 7.16 Load slip curves at the interior support for parametric study girders

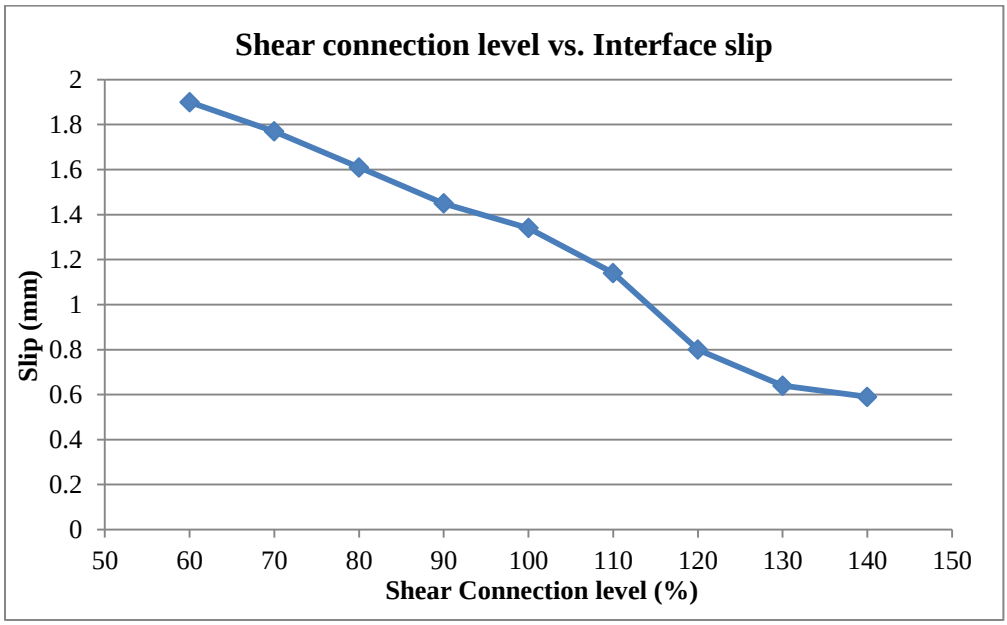

Figure 7.17 Relationship between shear connection level and slip at the interior support

7.6.3 CFRP Performance

In the parametric study girders, CFRP sheets are bonded to the top of concrete slab at negative moment region with same dimension used in the tested girders in addition to CFRP sheet used to wrap the concrete slab at positive moment region. Table 7.6 presents the CFRP strain values at yielding and ultimate loads for different girders. It is observed that the strain values are increased gradually with reducing of shear studs spacing at negative moment region. This is because the reducing of shear studs spacing allows providing more shear studs at negative moment region and increases the ability to transfer higher tangential shear force. Therefore, higher stress value develops in CFRP. At yielding load, the partial composite girders exhibit lower strain values than that attain by full composite girders (Figure 7.18).

The decreasing of shear studs spacing shifts the failure mode from crushing of concrete to de-bonding of CFRP. This is because the girders with higher shear connection level deflect more and the curvature increases over the interior support, so it allows developing higher strain values in CFRP. In addition, the increase of shear studs number at negative moment region gives CFRP the ability to generate higher strain values because the shear studs can transfer higher tangential shear force. Accordingly, the increase of CFRP strain reflects in higher stress value in the adhesive material and increase the opportunity to fail by de-bonding.

Table 7.6 CFRP strain at the interior support

Girder	CFRP Strain at Yielding Load (με)	CFRP Strain at Ultimate Load (με)
G-18.3	980	5840
G-15.7	1060	5990
G-13.8	1120	6070
G-12.2	1200	6130
G-11	1495	6210
G-10	1540	6310
G-9.2	1565	6400
G-8.5	1600	6480
G-7.8	1640	6550

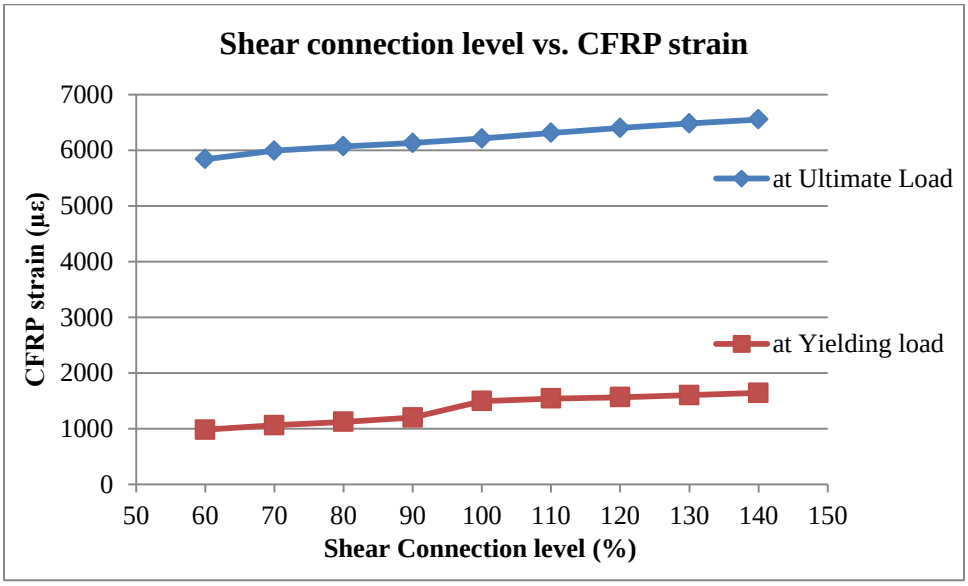

Figure 7.18 Relationship between shear connection level and CFRP strain

7.6.4 Parametric Study Conclusion

The design of shear studs at negative moment region using 40% of ultimate CFRP strain is appropriate to avoid de-bonding failure and conservatively estimates the ultimate load capacity of the composite girder. Also, the slip between concrete slab and steel beam remains within the acceptable limit according to design slip value. Depending on 40% of ultimate CFRP strain, 110mm is the proper shear studs spacing at negative moment region.

The tangential shear force should be transferred between concrete slab and steel beam is equal to the forces generate in CFRP and steel reinforcement (Figure 7.19), and the number of required shear studs is equal to the tangential shear force divided by nominal shear strength of shear studs. The following procedure shows the steps of shear studs design at negative moment region with presence of CFRP.

The tensile force generates in CFRP is equal to,

$$T_{CFRP} = (0.40\ \varepsilon_{u\ CFRP}) A_{CFRP}\ E_{CFRP} \tag{7.1}$$

And the force generated in steel reinforcement is equal to,

$$T_{S.R} = A_{S.R}\ F_{y\ S.R} \tag{7.2}$$

The total tangential shear force is equal to,

$$T_{max} = T_{CFRP} + T_{S.R} \tag{7.3}$$

The number of shear studs equals to,

$$No.of\ shear\ studs = T_{max}/Q_n \tag{7.4}$$

where Q_n is the nominal strength of shear studs.

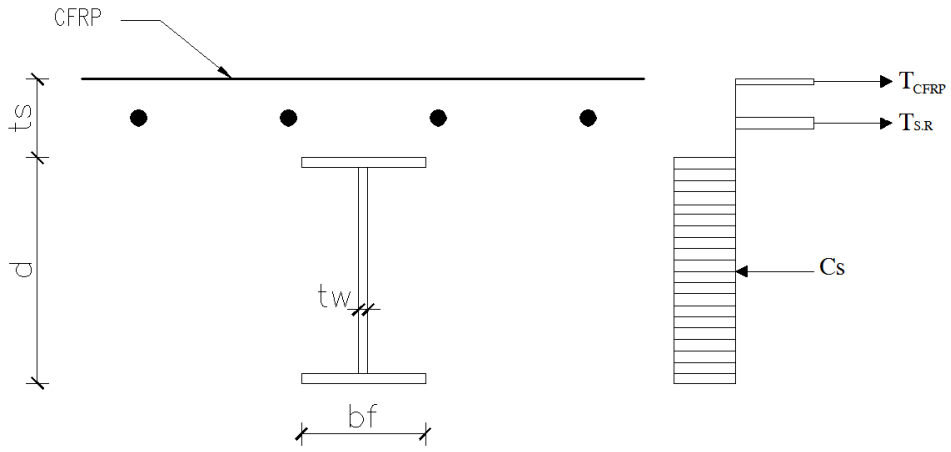

Figure 7.19 Composite girders cross section at negative moment region

CHAPTER 8

CONCLUSION AND RECOMMENDATIONS

8.1 Conclusion

The experimental work was carried out on continuous composite girders with variable shear studs spacing at negative moment regions. CFRP was bonded to the top of concrete slab at negative moment region. Three dimensional finite element models were created and analyzed using ABAQUS software and parametric study was carried out after validating the finite element results. The effects of shear studs spacing were discussed through load-deflection curves, interface slip, cracks distribution and propagation, and CFRP performance. From the experimental and numerical results the following conclusions are made.

1- For high level of shear connection, the continuous composite girders exhibit slight increase of stiffness.

2- The ultimate load capacity is not affected by the level of shear connection.

3- The increase of shear connection level reduces the interface slip between concrete slab and steel beam.

4- The contribution of CFRP to load resistance increases with high level of shear connection.

5- Shear studs at negative moment region are designed to transfer tensile forces of CFRP and steel reinforcement.

6- Tensile forces of CFRP sheets to be transferred by shear studs can be taken as 40% of CFRP ultimate capacity.

8.2 Recommendations

Following are some recommendations for future work.

1- Investigating the fatigue behavior of continuous steel-concrete composite girders strengthening with CFRP at negative moment region under cyclic loading.

2- Investigating the behavior of continuous composite girders by using different types of shear connectors like channel connectors.

3- Evaluating the performance of continuous composite girders by using Ultra High Performance Concrete (UHPC) instead of normal concrete at negative moment region.

References

ACI-Commetti-440. (2008). Guide for the Design and Construction of Externally Bonded FRP Systems for Strengthening Concrete Structures (ACI 440.2R-08): American Concrete Institute.

Basu, Prodyot K, Sharif, Alfarabi M, & Ahmed, Nesar U. (1987a). Partially prestressed composite beams. II. *Journal of Structural Engineering, 113*(9), 1926-1938.

Basu, Prodyot K, Sharif, Alfarabi M, & Ahmed, Nesar U. (1987b). Partially prestressed continuous composite beams. I. *Journal of Structural Engineering, 113*(9), 1909-1925.

Chen, Shiming, Wang, Xindi, & Jia, Yuanlin. (2009). A comparative study of continuous steel–concrete composite beams prestressed with external tendons: experimental investigation. *Journal of constructional steel research, 65*(7), 1480-1489.

Eurocode-4. (2005). Design of composite steel and concrete structures - Part 1-1: General rules and rules for buildings (Vol. EN 1994-1-1). Brussels.

Fabbrocino, G, & Pecce, M. (2000). *Experimental tests on steel–concrete composite beams under negative bending.* Paper presented at the 3rd structural specialty conference of the Canadian society for civil engineering. London (Ontario).

Hibbitt, K. (2013). ABAQUS: User's Manual: Version 6.13: Hibbitt. *Karlsson & Sorensen, Incorporated.*

Jankowiak, T, & Łodygowski, T. (2005). Identification of parameters of concrete damage plasticity constitutive model. *Foundations of Civil and Environmental Engineering*, 53-69.

Loh, HY, Uy, B, & Bradford, MA. (2004). The effects of partial shear connection in the hogging moment regions of composite beams: Part I—Experimental study. *Journal of Constructional Steel Research, 60*(6), 897-919.

Nguyen, Dai Minh, Chan, Toong Khuan, & Cheong, Hee Kiat. (2001). Brittle failure and bond development length of CFRP-concrete beams. *Journal of Composites for Construction, 5*(1), 12-17.

Nie, Jianguo, Fan, Jiansheng, & Cai, CS. (2008). Experimental study of partially shear-connected composite beams with profiled sheeting. *Engineering Structures, 30*(1), 1-12.

Nie, Jianguo, Tao, Muxuan, Cai, CS, & Li, Shaojing. (2011). Analytical and Numerical Modeling of Prestressed Continuous Steel-Concrete Composite Beams. *Journal of Structural Engineering*, *137*(12), 1405-1418.

Niu, Hedong, & Wu, Zhishen. (2006). Effects of FRP-concrete interface bond properties on the performance of RC beams strengthened in flexure with externally bonded FRP sheets. *Journal of materials in civil engineering*, *18*(5), 723-731.

Rosenboom, Owen, & Rizkalla, Sami. (2008). Modeling of IC debonding of FRP-strengthened concrete flexural members. *Journal of Composites for Construction*, *12*(2), 168-179.

Sharif, A, & Samaaneh, M. (2014). Modeling of continuous composite girders partially reinforced with CFRP,. *Concrete Solutions* 361.

Sharif, A, & Samaaneh, M. (2015). Use of CFRP to Maintain Composite Action of Continuous Composite Girders, *Deanship of Scientific Research* (Vol. III). King Fahd University of Petroleum and Minerals.

Spadea, G, Swamy, RN, & Bencardino, F. (2001). Strength and ductility of RC beams repaired with bonded CFRP laminates. *Journal of Bridge Engineering*, *6*(5), 349-355.

Ziraba, YN, Baluch, MH, Basunbul, IA, Sharif, AM, Azad, AK, & Al-Sulaimani, GJ. (1994). Guidelines toward the design of reinforced concrete (RC) beams with external plates. *ACI Structural Journal*, *91*(6).

VITAE

Name	Anas Mohammad Darwish
Place of Birth	Ramallah-Palestine
Date of Birth	21/1/1988
Permanent Address	Beitello-Ramallah-Palestine
Email	anas_dr88@yahoo.com
Phone Number	+970599034682 +966537061556

Academic Background

M.S (Civil Engineering-Structure)

King Fahd University of Petroleum and Minerals, Dhahran, Saudi Arabia

B.Sc. (Civil Engineering)

Birzeit University, Ramallah, Palestine